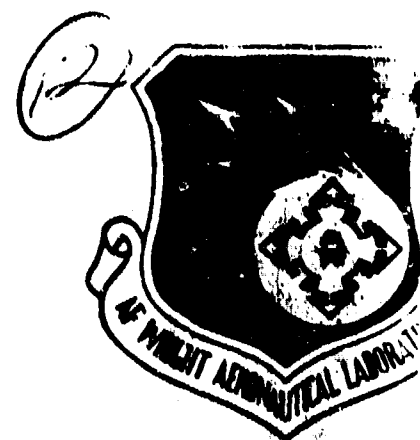


AFWAL-TR-83-3121
Volume I



LARGE DEFLECTION MULTIMODE RESPONSE OF CLAMPED
RECTANGULAR PANELS TO ACOUSTIC EXCITATION
VOLUME I

Chuh Mei

Department of Mechanical Engineering and Mechanics
School of Engineering
Old Dominion University
Norfolk, VA 23508

December 1983

Final Report for the period October 1, 1980 - May 31, 1983

APPROVED FOR PUBLIC RELEASE: DISTRIBUTION UNLIMITED

AD A139622



Flight Dynamics Laboratory
AF Wright Aeronautical Laboratories
Air Force Systems Command
Wright-Patterson AFB, Ohio 45433

84 04 03 007

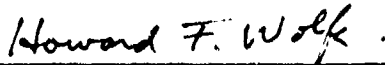
FILE COPY

NOTICE

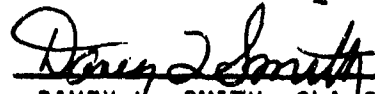
When Government drawings, specifications, or other data are used for any purpose other than in connection with a definitely related Government procurement operation the United States Government thereby incurs no responsibility nor any obligation whatsoever; and the fact that the government may have formulated, furnished, or in any way supplied the said drawings, specifications, or other data, is not to be regarded by implication or otherwise as in any manner licensing the holder or any other person or corporation, or conveying any rights or permission to manufacture use, or sell any patented invention that may in any way be related thereto.

This report has been reviewed by the Office of Public Affairs (ASD/PA) and is releasable to the National Technical Information Service (NTIS). At NTIS, it will be available to the general public, including foreign nations.

This technical report has been reviewed and is approved for publication.




HOWARD F. WOLFE
Project Monitor



DAVEY L. SMITH, Chief
Structural Integrity Branch
Structures & Dynamics Division

FOR THE COMMANDER



RALPH L. KUSTER, JR., COL, USAF
Chief, Structures & Dynamics Division

"If your address has changed; if you wish to be removed from our mailing list, or if the addressee is no longer employed by your organization please notify FIBED N-PAFB, OH 45433 to help us maintain a current mailing list".

Copies of this report should not be returned unless return is required by security considerations, contractual obligations, or notice on a specific document.

Unclassified

SECURITY CLASSIFICATION OF THIS PAGE (When Data Entered)

REPORT DOCUMENTATION PAGE		READ INSTRUCTIONS BEFORE COMPLETING FORM
1. REPORT NUMBER AFWAL-TR-83-3121 Volume I	2. GOVT ACCESSION NO. AD-A139622	3. RECIPIENT'S CATALOG NUMBER
4. TITLE (and Subtitle) LARGE DEFLECTION MULTIMODE RESPONSE OF CLAMPED RECTANGULAR PANELS TO ACOUSTIC EXCITATION VOLUME I		5. TYPE OF REPORT & PERIOD COVERED Final Technical Report October 1, 1980-May 31, 1983
7. AUTHOR(s) Chuh Mei		6. PERFORMING ORG. REPORT NUMBER
9. PERFORMING ORGANIZATION NAME AND ADDRESS Old Dominion University Research Foundation P. O. Box 6369 Norfolk, Virginia 23508		8. CONTRACT OR GRANT NUMBER(s) AFOSR-80-0107
11. CONTROLLING OFFICE NAME AND ADDRESS Flight Dynamics Laboratory (AFWAL/FIBED) AF Wright Aeronautical Laboratories, AFSC Wright-Patterson AFB, Ohio 45433		10. PROGRAM ELEMENT, PROJECT, TASK AREA & WORK UNIT NUMBERS 2307N119
14. MONITORING AGENCY NAME & ADDRESS (if different from Controlling Office)		12. REPORT DATE December 1983
		13. NUMBER OF PAGES 67
		15. SECURITY CLASS. (of this report) Unclassified
		15a. DECLASSIFICATION/DOWNGRADING SCHEDULE
16. DISTRIBUTION STATEMENT (of this Report) Approved for public release; distribution unlimited.		
17. DISTRIBUTION STATEMENT (of the abstract entered in Block 20, if different from Report)		
18. SUPPLEMENTARY NOTES AFWAL-TR-83-3121 Vol II contain computer software; therefore distribution is limited in accordance with AFR 300-6. Non-DOD requests must include the statement of terms and conditions in Atch 21 to AFR 300-6.		
19. KEY WORDS (Continue on reverse side if necessary and identify by block number) Nonlinear Random Vibrations Sonic Fatigue		
20. ABSTRACT (Continue on reverse side if necessary and identify by block number) An analytical method is developed for the determination of large deflec- tion multimodal random response of clamped rectangular plates subjected to normal incidence acoustic impingements. The Karman-Herrmann large deflection plate equations are solved by a technique which reduced the fourth order non- linear partial differential equations to a set of second order nonlinear differential equations with time as the independent variable. The differential equation solution utilizes a Fourier-type series representation of the areas ->		

DD FORM 1473

1 JAN 73

EDITION OF 1 NOV 65 IS OBSOLETE

1

Unclassified

SECURITY CLASSIFICATION OF THIS PAGE (When Data Entered)

Unclassified

SECURITY CLASSIFICATION OF THIS PAGE(When Data Entered)

→ function and out-of-plane deflection. The compatibility equation is solved by direct substitution, and the equilibrium equation is solved through the use of Bubnov-Galerkin method. The acoustic excitation is assumed to be Gaussian. The Krylov-Bogoliubov-Caughey equivalent linearization method is then employed that the derived set of second order nonlinear differential equations is linearized to an equivalent set of second order linear differential equations. Transformation of coordinates from the generalized displacements to the normal-mode coordinates and an iterative scheme are employed to obtain root-mean-square (RMS) maximum panel deflection, RMS maximum strain and equivalent linear (or nonlinear) frequencies of vibration for clamped rectangular panels at various excitation pressure spectral density (PSD). Convergence of the results is demonstrated by using 4, 6, 10 and 15 terms in the transverse deflection function. Effects of panel length-to-width ratio and damping ratio on panel response are also studied. There are two volumes reporting this research effort; this volume, Volume I, contains the mathematical formulations and numerical results, Volume II gives the computer program codes.

↑

Unclassified

SECURITY CLASSIFICATION OF THIS PAGE(When Data Entered)

FOREWORD

The project discussed in this technical report was performed under Grant AFOSR-80-0107 entitled "Large-Amplitude Multimode Response of Clamped Rectangular Panels to Acoustic Excitation." This document presents the results of analytical investigation into the behavior of plates acoustically loaded into the large deflection regime. There are two volumes reporting this research effort: Volume I consists of the mathematical formulations and numerical results; Volume II contains the computer codes. The study was conducted at the Department of Mechanical Engineering and Mechanics, Old Dominion University, Norfolk, Virginia. The work was monitored under the supervision of Howard F. Wolfe, AFWAL/FIBED, Technical Manager, Acoustics and Sonic Fatigue Group, Structural Integrity Branch, Structures and Dynamics Division, Flight Dynamics Laboratory of the Air Force Wright Aeronautical Laboratories, Wright-Patterson AFB, and Dr. Anthony K. Amos, AFOSR/NA, Program Administrator, Directorate of Aerospace Sciences, Bolling AFB.

The author wishes to acknowledge Howard F. Wolfe, Kenneth R. Wentz and Dr. Donald B. Paul for their encouragement and assistance. Also, the continued support of the effort by Dr. Anthony K. Amos made the accomplishment of this project possible.

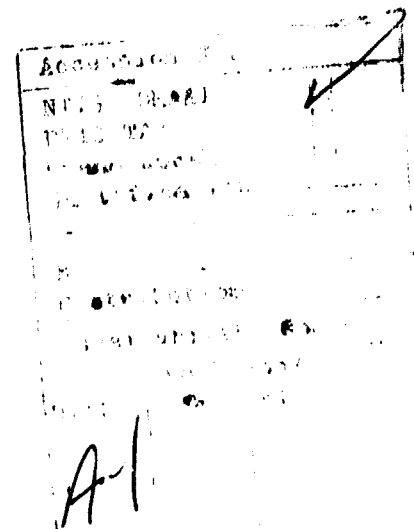


TABLE OF CONTENTS

SECTION	PAGE
I INTRODUCTION.....	1
1. Background.....	1
2. Objectives of the Investigation.....	3
II MATHEMATICAL FORMULATION AND SOLUTION PROCEDURE.....	4
1. Governing Equations.....	4
2. Solution.....	5
3. Deflection and Strains.....	27
III RESULTS AND DISCUSSION.....	30
1. General Comments.....	30
2. Convergence of the Nonlinear Random Response.....	31
3. Effects of Panel Damping.....	33
IV CONCLUDING REMARKS.....	42
APPENDIX A. INTEGRALS OF $\int_a^b \int_a^b L(w, F) f_r g_s dx dy$	45
APPENDIX B. EQUIVALENT LINEAR STIFFNESS MATRIX.....	49
REFERENCES.....	55

LIST OF FIGURES

FIGURE		PAGE
1	Coordinates and Dimensions.....	6
2	Lateral Deflection Term $f_1(x)g_1(y)$	10
3	Lateral Deflection Term $f_2(x)g_1(y)$	11
4	Lateral Deflection Term $f_1(x)g_2(y)$	12
5	Lateral Deflection Term $f_2(x)g_2(y)$	13
6	Lateral Deflection Term $f_3(x)g_1(y)$	14
7	Lateral Deflection Term $f_1(x)g_3(y)$	15
8	Band-Limited White Noise Excitation.....	32
9	Convergence of the Mean-Square Center Deflection for the Square Plate ($\zeta = 0.009$).....	34
10	Convergence of the Mean-Square Center Deflection for the Rectangular ($\alpha = 2$) Plate ($\zeta = 0.009$).....	35
11	Convergence of the Maximum Mean-Square Strain for the Square Plate ($\zeta = 0.009$).....	36
12	Convergence of the Maximum Mean-Square Strain for the Rectangular ($\alpha = 2$) Plate ($\zeta = 0.009$).....	37
13	Effects of Damping on Mean-Square Center Deflection for a Clamped Square Plate.....	38
14	Effects of Damping on Mean-Square Center Deflection for a Clamped Rectangular ($\alpha = 2$) Plate.....	39
15	Effects of Damping on Maximum Mean-Square Strain for a Clamped Square Plate.....	40
16	Effects of Damping on Maximum Mean-Square Strain for a Clamped Rectangular ($\alpha = 2$) Plate.....	41
17	Strain Response of a Square Aluminum Panel at Three Different Sound Pressure Levels.....	43

LIST OF TABLES

TABLE		PAGE
1	Generalized Displacements for Convergence Studies.....	31

NOMENCLATURE

a, b	length and width of plate
B_{pqankl}	integers defined by Equation (14)
$[C]$	generalized damping matrix
C_{pq}	function defined by Equation (69)
D	flexural rigidity
E	Young's modulus
f	frequency in Hz
$f_m(x), g_n(y)$	displacement functions defined by Equations (11, 12)
F	Airy stress function
F_{pq}	stress function coefficients defined by Equation (14)
h	thickness of plate
$i, j, k, l, m, n, p, q, r, s$	integers
$I_x(w_{mn}), I_y(w_{mn})$	functions defined by Equations (25, 26)
$[K]$	generalized stiffness matrix
L	mathematical operator defined by Equation (1)
$[M]$	generalized mass matrix
p	pressure
P	pressure in normal coordinates
P_x, P_y	average edge loads defined by Equations (29, 30)
q	normal coordinate
S_f	dimensionless pressure spectral density defined by Equation (61)

NOMENCLATURE - CONTINUED

$S_p(\omega)$	spectral density of $P(t)$
t	time
u, v	inplane displacements
w	lateral deflection
W_{mn}	generalized displacements
x, y	coordinates
$Z_x(W_{mn}), Z_y(W_{mn})$	functions defined by Equations (27, 28)
α	length-to-width ratio, a/b
β	vector function defined by Equations (33, A6-A8, B2)
γ	shearing strain
ϵ	normal strain
ζ	damping ratio, c/c_c
μ	mass parameter defined by Equation (64)
ν	Poisson's ratio
ρ	mass density
σ	normal stress
τ	shearing stress
ϕ	normal mode
ω	linear frequency in rad/sec
Ω	equivalent linear or nonlinear frequency in rad/sec
<u>Subscripts</u>	
b	bending component
EL	equivalent linear
L	linear
o	membrane component

SECTION I

INTRODUCTION

1. BACKGROUND

Acoustically induced fatigue failures in aircraft and missile operation have been a design consideration for over 25 years. The problem was introduced with the advent of the turbo jet engine which produced high intensity acoustic pressure fluctuations on aircraft surfaces. As the engine performance requirements increased, the intensity of the acoustic pressures increased. Airframe minimum weight requirements resulted in higher stresses in structural components. The number of acoustic fatigue failures began to grow at a rapid rate until adequate design criteria were developed and used in the design process.

Similar fatigue failures have occurred in other regions of high intensity pressure fluctuations. These have occurred in regions of separated flow, behind protuberances into the flow such as airbrakes, and close to propeller tips. Failures have also occurred from the fluctuating pressure induced when bomb bay doors are opened during high speed flight.

The oscillating pressures from various noise sources produced a resonant response of the structural component such as external skin panels, frames, ribs and spars which results in rapid stress reversals in the structure. If these stresses have sufficient magnitude, fatigue failures occur.

Acoustic fatigue failures have resulted in unacceptable maintenance and inspection burdens associated with the operation of the aircraft. In some cases, sonic fatigue failures have resulted in major redesign efforts of aircraft structural components. Therefore, accurate prediction methods are

needed to determine the acoustic fatigue life of structures. Many analytical and experimental programs to develop sonic fatigue design criteria, however, have repeatedly shown a poor comparison between analytical and measured RMS maximum strain (References 1-9). Deviations in excess of 100 percent are not uncommon. One of the major reasons suspected for the discrepancy was that the panel response was based on small deflection linear structural theory, whereas the test panels responded with large deflections at high sound pressure levels (SPL).

Most recently, an analytical effort (References 10, 11) using a single-mode approach, and a test program (Reference 12) have demonstrated that the prediction of panel random response is greatly improved by the inclusion of large deflection effects in the analysis.

Test results in References 1, 2 and 12 also have shown that there are more than one mode responding. Multiple modes were also observed by Wolfe and Wentz (Reference 13) and White (Reference 14) in experimental investigations on aluminum fuselage panels and carbon fiber-reinforced plastics (CFRP) plates under acoustic loading. White also showed that the fundamental mode responded significantly and contributed more than one-half of the total mean-square strain response; higher modes, up to third or fourth modes, account for 95% or more of the total mean-square strain response. In order to have an accurate determination of the random response of a structure, multiple modes should be used in the analysis. This report, Volume I, presents an analytical effort on large-amplitude random response of a clamped rectangular thin plate subjected to acoustic excitation using multiple (4) modes in the formulation. The developed computer software is published in Volume II of this document.

2. OBJECTIVES OF THE INVESTIGATION

The primary aim of this research is to investigate the large-amplitude, multimodal response of clamped, rectangular, flat, thin panels of uniform thickness subjected to broadband, random acoustic excitation. More specifically, the following tasks will be performed in accomplishing this aim:

- (a) Development of an "quasi-exact" solution procedure for determining the nonlinear response of a clamped rectangular plate to random loading;
- (b) Computerization of the solution procedure to simplify application to the nonlinear random response problems studied in this investigation and for the convenience of other researchers who wish to use and/or extend this work; and
- (c) Determination of the RMS maximum panel deflection, the RMS maximum strain, and the frequencies of vibration of an acoustically excited clamped plate which will enable the practical utilization for estimation of sonic fatigue life.

SECTION II

MATHEMATICAL FORMULATION AND SOLUTION PROCEDURE

1. GOVERNING EQUATIONS

The governing equations of a thin rectangular, isotropic plate undergoing large-deflection motions, neglecting the effects of both inplane and rotatory inertia forces, are (References 15, 16)

$$\begin{aligned}
 L(w, F) = & DV^4w + \rho h w_{,tt} + g w_{,t} \\
 & - h(F_{,yy} w_{,xx} + F_{,xx} w_{,yy} - 2 F_{,xy} w_{,xy}) \\
 & - p(t) = 0
 \end{aligned} \tag{1}$$

$$V^4 F = E(w_{,xy}^2 - w_{,xx} w_{,yy}) \tag{2}$$

where a comma denotes the partial differentiation with respect to the corresponding variable, w is the lateral deflection, D is the flexural rigidity, ρ is the mass density, h is the plate thickness, p is the pressure, E is the Young's modulus, and g is the viscous damping. The stress function F is defined by

$$\sigma_{ox} = F_{,yy} \tag{3}$$

$$\sigma_{oy} = F_{,xx} \tag{4}$$

$$\tau_{oxy} = -F_{,xy} \tag{5}$$

where σ_{ox} , σ_{oy} and τ_{oxy} are the membrane stresses.

Equations (1) and (2) together with a complete set of boundary conditions, define the problem. These equations are subjected to the usual out-of-plane boundary conditions required in small deflection theory (zero edge deflection and slope for clamped edges). In addition, for large deflections, it is necessary to specify inplane boundary conditions. The inplane boundary conditions must be specified in terms of a combination of applied edge load and displacements.

The particular inplane boundary conditions of most interest in the study of sonic fatigue of structural panels is the one in which the edges are restrained from movement, that is

$$u = 0 \quad \text{on } x = 0 \text{ and } a \quad (6)$$

$$v = 0 \quad \text{on } y = 0 \text{ and } b \quad (7)$$

where the plate has a length a , width b , and the origin of the coordinates is taken at one corner as indicated in Figure 1. The numerical results presented in the next section are all based on these inplane boundary conditions.

2. SOLUTION

Generally, there are four methods which are used in the analysis of multi-degree-of-freedom nonlinear systems under random excitations. These are the Fokker-Planck equation approach, the perturbation approach, the finite difference approach and the equivalent (statistical or stochastic)

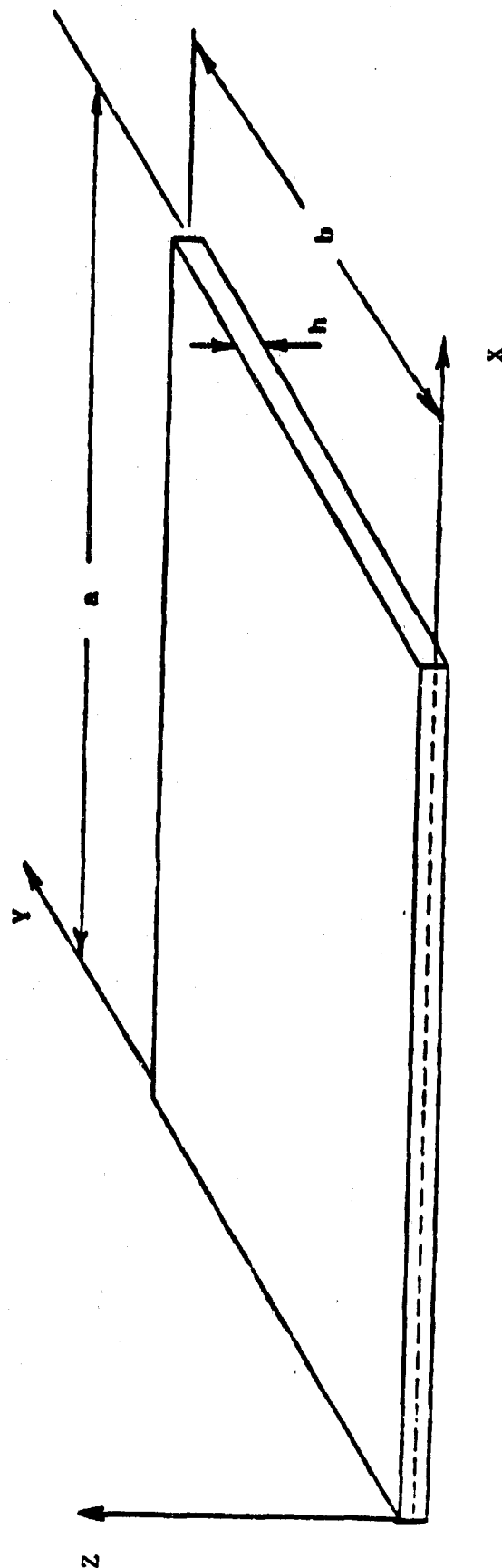


Figure 1. Coordinates and Dimensions

linearization approach. Application of these methods to panels of complex configurations were discussed in Reference 4. There have been very few attempts at solution of Equations (1) and (2) treating plates under random loading.

The classical approach attempts a direct solution of the differential equations, thereby allowing a reduction in numerical approximations. This approach generally involves the assumption of a set of global solution functions which are simple analytically, usually one term (References 10, 11, 17 and 18) and satisfy the geometric boundary conditions. The differential equations are then satisfied approximately by use of a Rayleigh-Ritz or Galerkin procedure. Such an approach allows simple solutions; but since the shape of the solution functions are predetermined, the accuracy of the prediction is limited by these choices. A complete description of the deflection shape will not be able to emerge since the shape has been predetermined. A notable exception to the constrained function approach was the solution procedure developed by Levy (Reference 19) for bending of a simply supported rectangular plate with large deflections.

Levy's procedure involved the representation of the stress function F and the lateral deflection function w by double infinite Fourier series. Such a representation of the solution functions by a complete set of "basic functions" removes the major limitation of constrained solution functions present in the earlier solutions. The relationship between the coefficients of the stress function series and the lateral deflection function series was determined by direct substitution of the two series into the compatibility equation and by equating coefficients of like trigonometric terms. The equilibrium equation was then solved by the same procedure of substitution

of the two series for F and w into the equilibrium equation and equating coefficients of like trigonometric terms. The result of these operations was an infinite set of simultaneous algebraic equations which were cubic in the deflection function coefficients. This set of equations represents a complete solution of the large deflection plate bending equations for the simply supported rectangular plate. Levy's solution is referred to as an "exact" solution by Timoshenko (Reference 15) and other authors. Of course, the exact numerical results cannot be obtained (this would require solution of an infinite number of simultaneous equations), but since the series is complete and the solution convergent, the degree of accuracy of the results depends only on the patience and time of the analyst. Levy's solution procedure has been very useful to the research community as evidenced by the many investigators which have made use of and extended his solution to study various phenomena associated with the large deflection of plates. For example, Paul (Reference 20) extended Levy's procedure to study large deflection behavior of clamped plates under thermal loading. The representation of the stress function and the plate deflection function which is developed herein will also follow the same procedure as Levy and Paul.

The solution will be written in terms of the stress function F and the lateral displacement w , with the relationship between these variables determined by satisfying the compatibility equation, Equation (2). The lateral deflection w is represented by a complete set of functions in the form of a "Fourier-type" double series.

$$w(x,y,t) = h \sum_m \sum_n W_{mn}(t) f_m(x) g_n(y) \quad m,n = 1,2,3... \quad (8)$$

The functions $f_m(x)$ and $g_n(y)$ are chosen to be linearly independent of each other and such that the geometric boundary conditions of zero slope and deflection along the edges of the plate are satisfied exactly. The $W_{mn}(t)$ are the generalized displacements which are to be determined. The lateral boundary conditions are

$$w = w_x = 0 \quad \text{on } x = 0 \text{ and } a \quad (9)$$

$$w = w_y = 0 \quad \text{on } y = 0 \text{ and } b \quad (10)$$

The functions $f_m(x)$ and $g_n(y)$ which meet the above requirements are given by:

$$f_m(x) = \cos\left(\frac{(m-1)\pi x}{a}\right) - \cos\left(\frac{(m+1)\pi x}{a}\right) \quad (11)$$

and

$$g_n(y) = \cos\left(\frac{(n-1)\pi y}{b}\right) - \cos\left(\frac{(n+1)\pi y}{b}\right) \quad (12)$$

To help perceive the numerical behavior for the component functions $f_m(x)$ and $g_n(y)$ which make up the series, the first six terms of the series (Equation 8) are shown in Figures 2 through 7. These figures are plotted with the generalized displacement W_{mn} held constant.

Upon examination of the above expression of the lateral deflection, it is found that the compatibility equation (Equation 2) can be identically satisfied if the stress function F is taken in the following form:

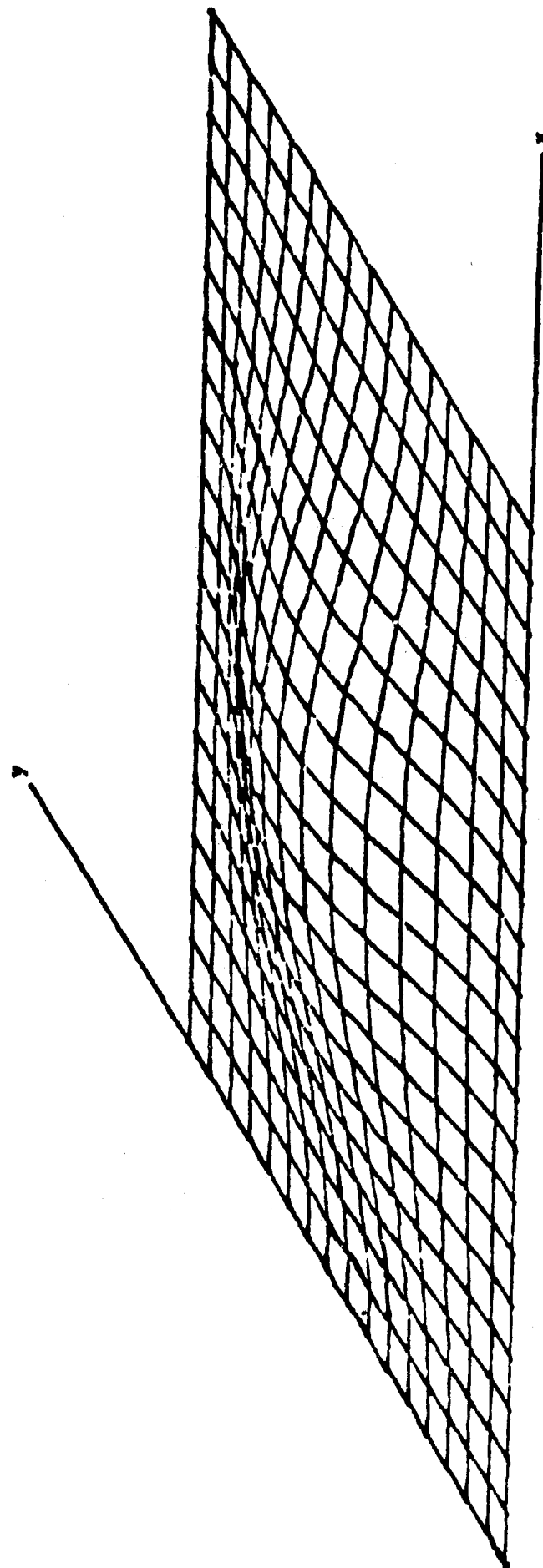


Figure 2. Lateral Deflection Term $f_1(x)g_1(y)$

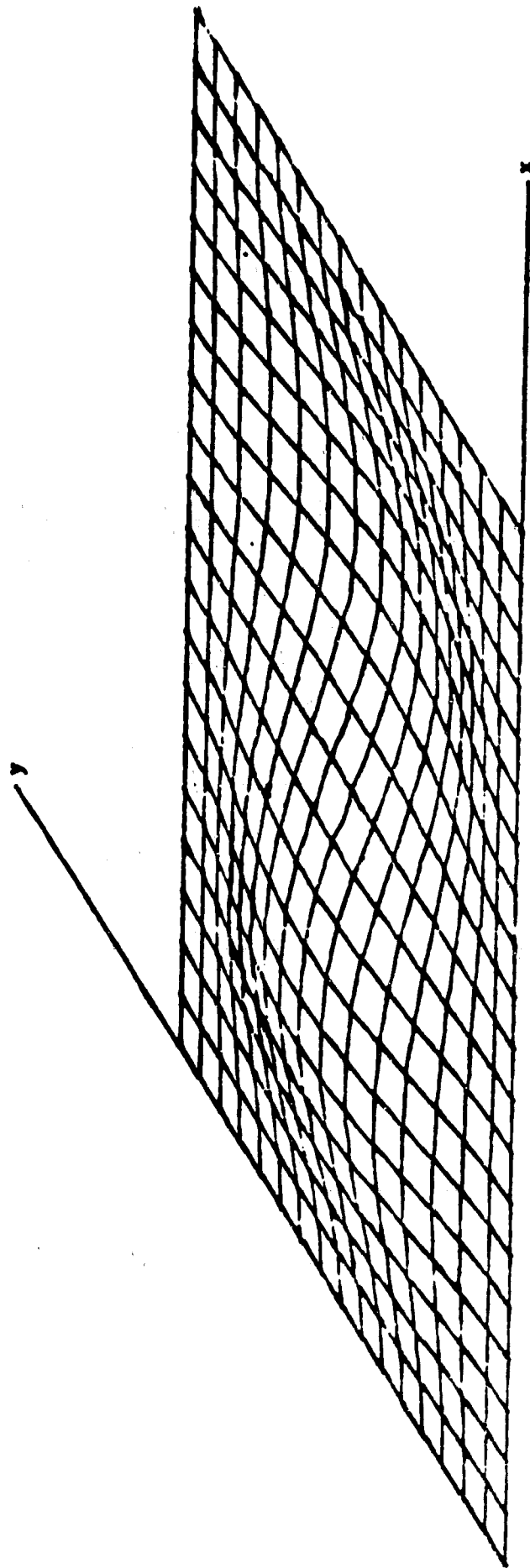


Figure 3. Lateral Deflection Term $f_2(x)g_1(y)$

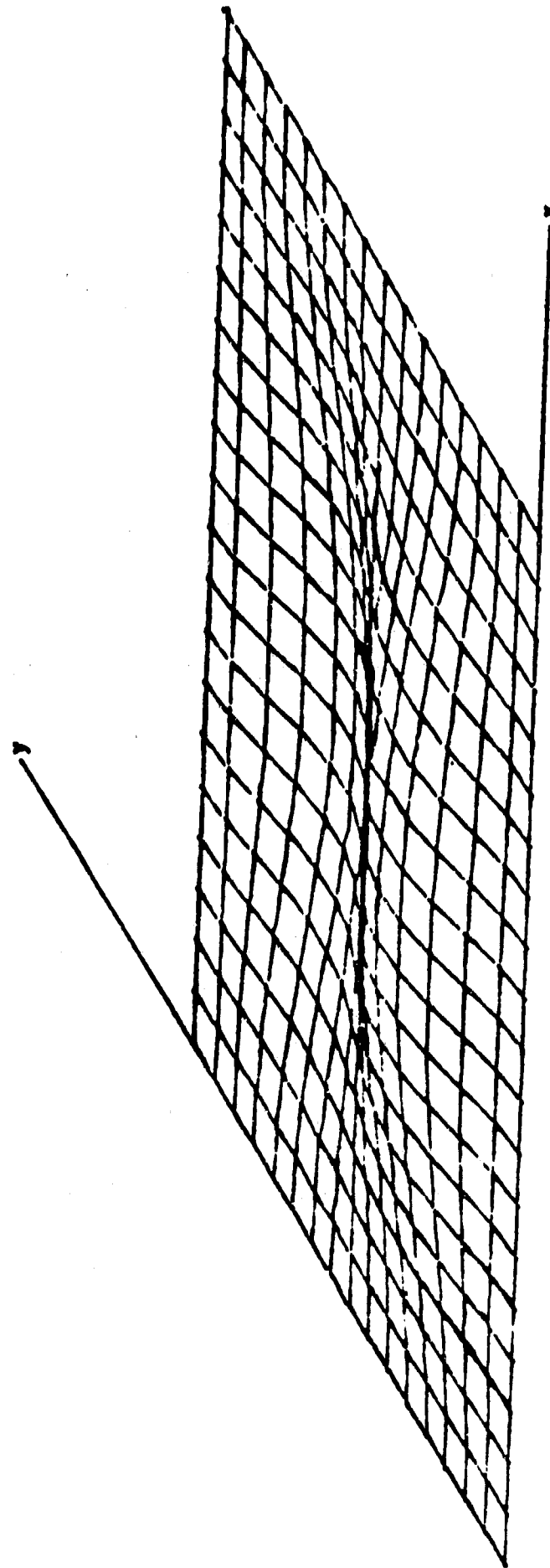


Figure 4. Lateral Deflection Term $f_1(x)g_2(y)$

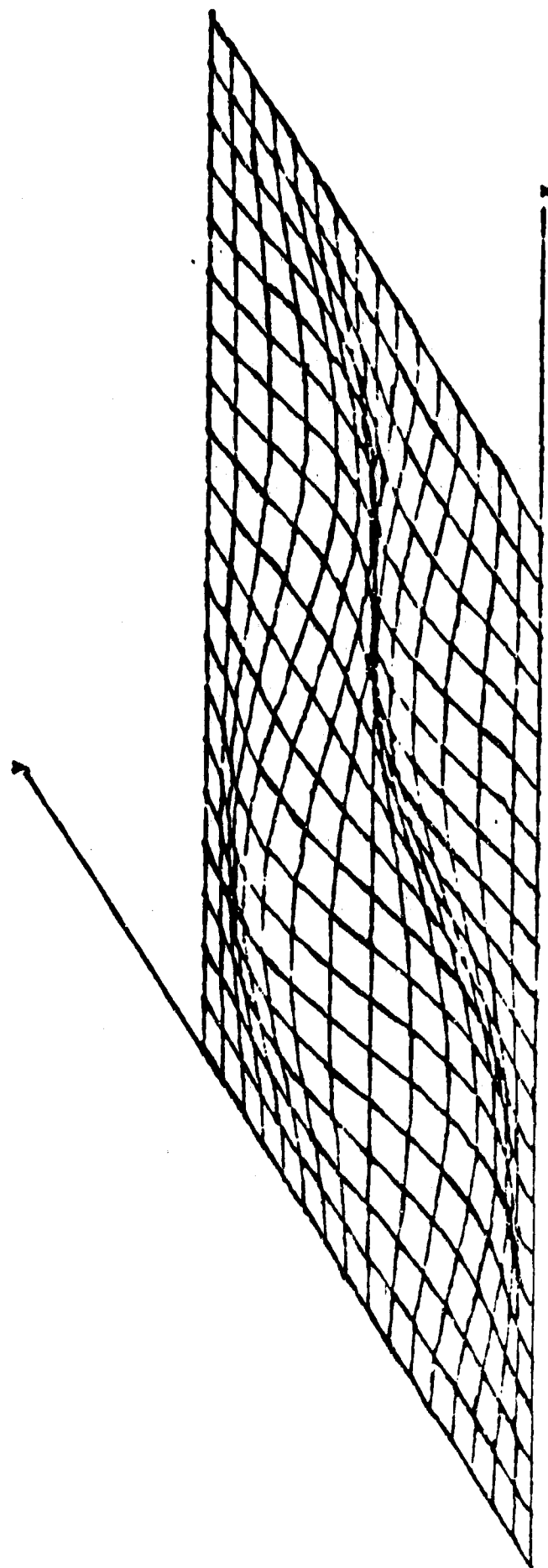


Figure 5. Lateral Deflection Term $f_2(x)g_2(y)$

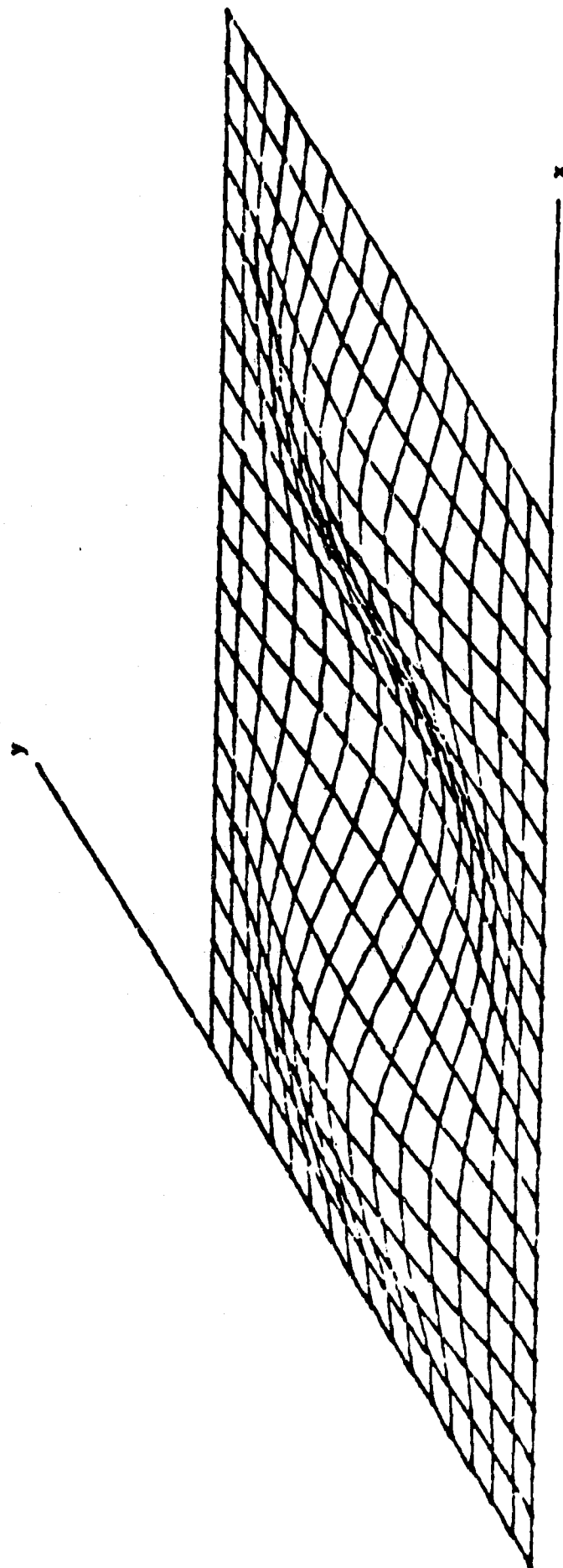


Figure 6. Lateral Deflection Term $f_3(x)g_1(y)$

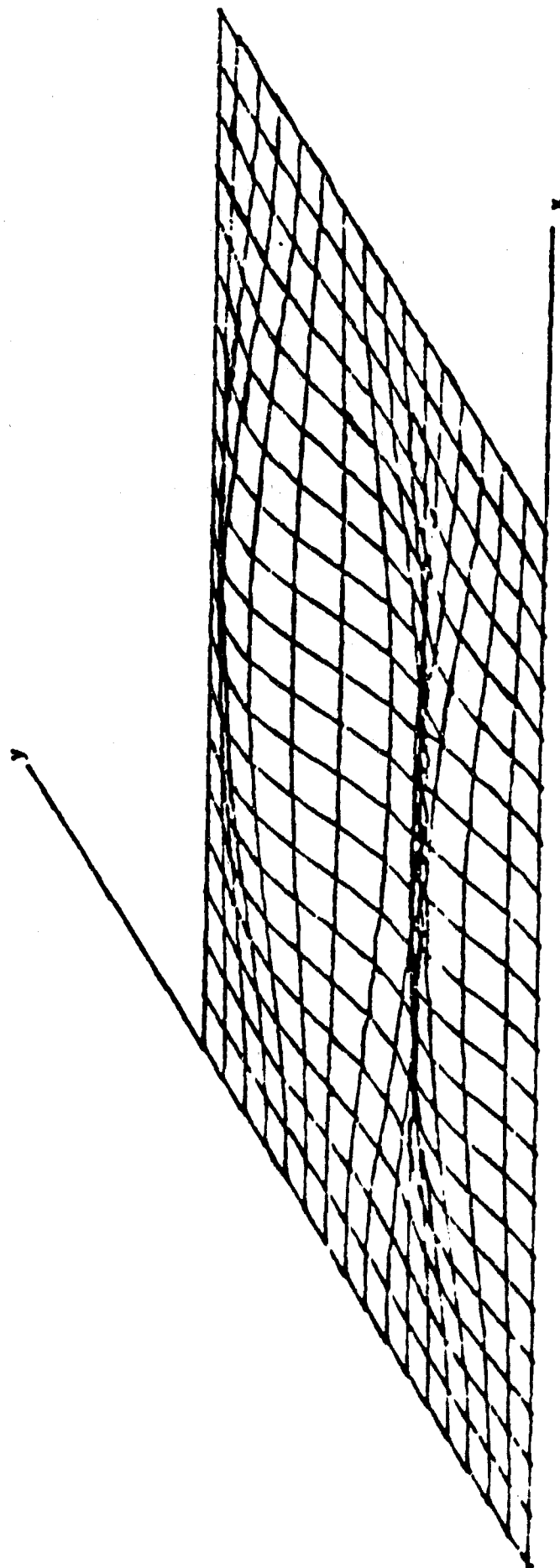


Figure 7. Lateral Deflection Term $f_1(x)g_3(y)$

$$F = -\frac{P_x y^2}{2} - \frac{P_y x^2}{2} + Eh^2 \sum_p \sum_q F_{pq} \cos\left(\frac{p\pi x}{a}\right) \cos\left(\frac{q\pi y}{b}\right) \quad p, q = 0, 1, 2, \dots \quad (13)$$

where the constants P_x and P_y contribute to the membrane stress and will be discussed in more detail later. Also, it should be noted that the above form of the stress function implies zero shear stress on the plate boundaries. Direct substitution of Equations (8, 11, 12 and 13) into the compatibility equation Equation (2), performing the required differentiations and multiplications, and equating coefficients of like trigonometric terms yields the following quadratic relationship between F_{pq} and W_{mn}

$$F_{pq} = \frac{1}{(p^2/\alpha + q^2\alpha)^2} \sum_m \sum_n \sum_k \sum_l B_{pqmnkl} W_{mn} W_{kl} \quad (14)$$

where B_{pqmnkl} are integers and $\alpha = a/b$. Derivation of B_{pqmnkl} can be found in detail in Reference 20. The calculation of the integers B_{pqmnkl} is accomplished with the aid of a computer program, a listing of which is presented in Volume II of the report. A tabulation of B_{pqmnkl} for values of the subindices p, q, m, n, k and l from zero through nine has been generated, but it is too voluminous to be included in the report. However, a sample of this tabulation can be found in Reference 20. Substitution of Equation (14) into Equation (13) yields the following expression for the stress function in terms of the unknown parameters W_{mn} ,

$$F = -\frac{P_x y^2}{2} - \frac{P_y x^2}{2} + Eh^2 \sum_p \sum_q \left[\right.$$

$$\frac{1}{(p^2/a + q^2a)^2} \sum_m \sum_n \sum_k \sum_l B_{pqmnkl} W_{mn} W_{kl} \Big] \cos \frac{p\pi x}{a} \cos \frac{q\pi y}{b}$$

$$p, q = 0, 1, 2, \dots$$

$$m, n, k, l = 1, 2, 3, \dots \quad (15)$$

In the above equation, the P_x and P_y are determined by applying the in-plane boundary conditions, and the W_{mn} are determined by solving the remaining governing differential Equation (1).

As stated earlier, the numerical results presented in this study are based on the case in which the edges are restrained from movement (Equations 6 and 7). In order to apply these inplane boundary conditions, expressions for the inplane displacement must be developed. Combining the membrane strain-displacement relations

$$\epsilon_{ox} = u_{,x} + \frac{1}{2} w_{,x}^2 \quad (16)$$

$$\epsilon_{oy} = v_{,y} + \frac{1}{2} w_{,y}^2 \quad (17)$$

$$\gamma_{oxy} = u_{,y} + v_{,x} + w_{,x} w_{,y} \quad (18)$$

and the membrane strain-stress relations

$$\epsilon_{ox} = \frac{1}{E} (F_{,yy} - \nu F_{,xx}) \quad (19)$$

$$\epsilon_{oy} = \frac{1}{E} (F_{,xx} - \nu F_{,yy}) \quad (20)$$

and re-arrangement of the resulting expressions yield

$$\int_0^a \frac{\partial u}{\partial x} dx = \int_0^a \left[\frac{1}{E} (F_{,yy} - \nu F_{,xx}) - \frac{1}{2} w_{,x}^2 \right] dx \quad (21)$$

$$\int_0^b \frac{\partial v}{\partial y} dy = \int_0^b \left[\frac{1}{E} (F_{,xx} - \nu F_{,yy}) - \frac{1}{2} w_{,y}^2 \right] dy \quad (22)$$

where E is the Young's modulus and ν is the Poisson's ratio.

Performing the indicated differentiation, integration and applying the in-plane boundary condition (Equations 6, 7) to each of the above equations respectively yield:

$$0 = -\frac{P_x a}{E} + \frac{\nu P_y a}{E} - I_x(w_{mn}) \quad (23)$$

$$0 = -\frac{P_y b}{E} + \frac{\nu P_x b}{E} - I_y(w_{mn}) \quad (24)$$

The terms $I_x(w_{mn})$ and $I_y(w_{mn})$ in the above equations are defined by

$$I_x(w_{mn}) = \frac{h^2 \pi^2}{8a} \sum_m \sum_n w_{mn} z_x(w_{mn}) \quad (25)$$

$$I_y(w_{mn}) = \frac{h^2 \pi^2}{8b} \sum_m \sum_n w_{mn} z_y(w_{mn}) \quad (26)$$

$$\begin{aligned}
Z_x(W_{mn}) = & [(m+1)^2 + (m-1)^2]W_{m,2-n} - (m+1)^2W_{m+2,2-n} \\
& - (m-1)^2W_{m-2,2-n} + 2[(m+1)^2 + (m-1)^2]W_{mn} \\
& - 2(m+1)^2W_{m+2,n} - 2(m-1)^2W_{m-2,n} \\
& - [(m+1)^2 + (m-1)^2]W_{m,n-2} + (m+1)^2W_{m+2,n-2} \\
& + (m-1)^2W_{m-2,n-2} - [(m+1)^2 + (m-1)^2]W_{m,n+2} \\
& + (m+1)^2W_{m+2,n+2} + (m-1)^2W_{m-2,n+2}
\end{aligned} \tag{27}$$

$$\begin{aligned}
Z_y(W_{mn}) = & [(n+1)^2 + (n-1)^2]W_{2-m,n} - (n+1)^2W_{2-m,n+2} \\
& - (n-1)^2W_{2-m,n-2} + 2[(n+1)^2 + (n-1)^2]W_{mn} \\
& - 2(n+1)^2W_{m,n-2} - 2(n-1)^2W_{m,n+2} \\
& - [(n+1)^2 + (n-1)^2]W_{m-2,n} + (n+1)^2W_{m-2,n+2} \\
& + (n-1)^2W_{m-2,n-2} - [(n+1)^2 + (n-1)^2]W_{m+2,n} \\
& + (n+1)^2W_{m+2,n+2} + (n-1)^2W_{m+2,n-2}
\end{aligned} \tag{28}$$

where $W_{mn} = 0$ for m or $n < 1$.

Solving Equations (23) and (24) simultaneously yields the following expressions for the average edge loads P_x and P_y for the inplane boundary conditions in which the edges are restrained from movement

$$P_x = - \frac{E}{1-\nu^2} \left(\frac{\nu}{b} I_y + \frac{1}{a} I_x \right) \quad (29)$$

$$P_y = - \frac{E}{1-\nu^2} \left(\frac{\nu}{a} I_x + \frac{1}{b} I_y \right) \quad (30)$$

With the lateral deflection given by Equation (8) and the stress function given by Equation (15), the equilibrium equation, Equation (1), is then satisfied by applying the Bubnov-Galerkin method (Reference 21)

$$\int_0^b \int_0^a L(w, F) f_r g_s dx dy = 0 \quad r, s = 1, 2, 3, \dots \quad (31)$$

Upon substitution of $L(w, F)$ in Equation (31), the equations are written as

$$\begin{aligned} \int_0^b \int_0^a \{ \rho h w_{,tt} + g w_{,t} + D(w_{,xxxx} + 2w_{,xxyy} + w_{,yyyy}) \\ - h(F_{,yy} w_{,xx} + F_{,xx} w_{,yy} - 2F_{,xy} w_{,xy}) - p \} f_r g_s dx dy = 0 \end{aligned}$$

$$\text{where } r, s = 1, 2, 3, \dots \quad (32)$$

Utilizing the expressions for w , f_r , g_s and F (Equations 8, 11, 12

and 15, respectively) and performing the above integrations yield a set of second order nonlinear differential equations for the generalized displacements with time as the independent variable, and it can be written in matrix notation as

$$[M] \{\ddot{W}\} + [C] \{\dot{W}\} + [K]_L \{W\} + \{\beta(W)\} = \{p(\tau)\} \quad (33)$$

where $[M]$, $[C]$ and $[K]_L$ are the generalized mass, damping and linear stiffness matrices, respectively, and $\{\beta(W)\}$ is a vector function which is cubic in the generalized displacements $\{W\}$. The integrations of each of the terms in Equation (32) are given explicitly in Appendix A. The mass and linear stiffness matrices can be easily generated from equations (A1) to (A4).

If the acoustic pressure loading $p(t)$ is stationary Gaussian, is ergodic and has a zero mean. Application of the Krylov-Bogoliubov-Caughey equivalent linearization method (References 22-28) yields an equivalent set of linearized equations to Equation (33) as

$$[M] \{\ddot{W}\} + [C] \{\dot{W}\} + ([K]_L + [K]_{EL}) \{W\} = \{p(t)\} \quad (34)$$

or

$$[M] \{\ddot{W}\} + [C] \{\dot{W}\} + [K] \{W\} = \{p(t)\} \quad (35)$$

where $[K]_{EL}$ is the generalized equivalent linear stiffness matrix and $[K] = [K]_L + [K]_{EL}$. The elements of $[K]_{EL}$ are evaluated from the equation (Reference 23)

$$(K_{EL})_{rsij} = \xi \left[\frac{\partial \beta}{\partial W_{ij}} \right]_{rs} \quad (36)$$

and they are derived and given explicitly in Appendix B, and $\xi[\]$ stands for the operator of mathematical expectation. The approximate generalized displacements $\{W\}$, computed from the linearized equation, Equation (35), are also Gaussian and approach stationary because the panel motion is stable.

To determine the mean-square generalized displacements $\overline{W_{mn}^2}$ in Equation (34), an iterative process is introduced. The undamped linear equation of Equation (34) is solved first, which requires the determination of the eigenvalues and eigenvectors of the undamped linear equation

$$\omega_j^2 [M] \{\phi\}_j = [K]_L \{\phi\}_j \quad (37)$$

where ω_j is the linear frequency of vibration, and $\{\phi\}_j$ is the normal mode shape.

Apply a coordinate transformation, from the generalized displacements to the normal coordinates (4 modes will be used in the analysis, $n = 4$), by

$$\begin{matrix} \{W\} &= & [\phi] \{q\} & n \leq m \\ mx1 & & mxn \ nx1 & \end{matrix} \quad (38)$$

where each column of $[\phi]$ is a normal mode $\{\phi\}_j$. The damped linear equation of Equation (34) becomes

$$[M] \ddot{q} + [C] \dot{q} + [K]_L q = \{P(t)\} \quad (39)$$

$$\text{where } [M] = [\phi]^T [M] [\phi] \quad (40)$$

$$[C] = [\phi]^T [C] [\phi] = 2 [\zeta \omega] [M] \quad (41)$$

$$[K]_L = [\phi]^T [K]_L [\phi] = [\omega^2] [M] \quad (42)$$

$$\{P\} = [\phi]^T \{p\} \quad (43)$$

Equation (39) is uncoupled in the normal coordinates, the j th row of Equation (39) is

$$\ddot{q}_j + 2 \zeta_j \omega_j \dot{q}_j + \omega_j^2 q_j = \frac{P_j}{M_j} \quad (44)$$

The mean-square response of modal amplitude is

$$\overline{q_j^2} = \int_0^\infty S_p(\omega) |H_j(\omega)|^2 d\omega \quad (45)$$

where $S_p(\omega)$ is the spectral density function of the excitation $P_j(t)$, and the frequency response function is given by

$$H_j(\omega) = \frac{1}{M_j(\omega_j^2 - \omega^2 + 2i\zeta_j\omega_j\omega)} \quad (46)$$

For lightly damped ($\zeta = c/c_c \leq 0.05$) structures, the response curves will be highly peaked at ω_j . The integration of Equation (45) can be greatly simplified if the forcing spectral density function $S_p(\omega)$ can be considered to be constant in the frequency band surrounding the linear resonance peak ω_j , so that

$$\overline{q_j^2} \approx \frac{\pi S_p(\omega_j)}{4M_j^2 \zeta_j \omega_j^3} \quad (47)$$

The covariance matrix of the linear generalized displacements is

$$\overline{[W_{mn} W_{kl}]_L} = \frac{\pi}{4} \sum_j \{\phi\}_j \frac{S_p(\omega_j)}{M_j^2 \zeta_j \omega_j^3} \{\phi\}_j^T \quad (48)$$

The diagonal terms of $\overline{[W_{mn} W_{kl}]_L}$ are the mean-square linear generalized displacements $\overline{w_{mn}^2}$. This initial estimate of expected value on generalized displacements now can be used to compute the generalized equivalent linear stiffness matrix $[K]_{EL}$ through Equation (36) or Equations (B4 to B7). The undamped linearized equation of Equation (34) is solved again

$$\Omega_j^2 [M] \{\phi\}_j = ([K]_L + [K]_{EL}) \{\phi\}_j \quad (49)$$

where Ω_j is the equivalent linear or nonlinear frequency of vibration, and

$\{\phi\}_j$ is the associated equivalent linear normal mode. Then Equation (35) is transformed again to the normal coordinates and it has the form as

$$\Gamma M \downarrow \{\ddot{q}\} + \Gamma C \downarrow \{\dot{q}\} + \Gamma K \downarrow \{q\} = \{P(t)\} \quad (50)$$

in which

$$\Gamma K \downarrow = \{\phi\}^T ([K]_L + [K]_{EL}) \{\phi\} = \Gamma \Omega^2 \downarrow \Gamma M \downarrow \quad (51)$$

The j th row of Equation (50) is

$$\ddot{q}_j + 2\zeta_j \omega_j \dot{q}_j + \Omega_j^2 q_j = \frac{P_j}{M_j} \quad (52)$$

and the displacement covariance matrix is

$$\overline{[W_{mn} W_{kl}]} = \frac{\pi}{4} \sum_j \{\phi\}_j \frac{S_P(\Omega_j)}{M_j^2 \zeta_j \omega_j \Omega_j^2} \{\phi\}_j^T \quad (53)$$

The diagonal terms of $\overline{[W_{mn} W_{kl}]}$ are the mean-square generalized displacements $\overline{W_{mn}^2}$. As the iterative process converges on the $iter$ -th cycle, the relations

$$\overline{(q_j^2)}_{iter} \cong \overline{(q_j^2)}_{iter-1} \quad (54)$$

$$(\Omega_j)_{\text{iter}} = (\Omega_j)_{\text{iter}-1} \quad (55)$$

$$\overline{(w_{mn}^2)}_{\text{iter}} = \overline{(w_{mn}^2)}_{\text{iter}-1} \quad (56)$$

become satisfied. In the numerical results presented in the following section, convergence is considered achieved when the difference of the RMS displacements satisfies the relation

$$\left| \frac{(\text{RMS } w_{mn})_{\text{iter}} - (\text{RMS } w_{mn})_{\text{iter}-1}}{(\text{RMS } w_{mn})_{\text{iter}}} \right| < 10^{-3} \text{ for all } m, n \quad (57)$$

Once the RMS generalized displacements are determined, the RMS deflection of the panel and the RMS maximum strain can be determined from Equations (8, 19, 20) and the bending strain-displacement relations as presented in the next section.

In practice, the spectral density is usually given or measured in terms of the frequency f in Hertz. To convert the spectral density from the analytical $S_p(\omega)$ to practical $S_p(f)$, the following relations are used (Reference 29)

$$\omega = 2\pi f \quad (58)$$

$$S_p(\omega) = S_p(f)/2\pi \quad (59)$$

The pressure spectral density function $S_p(f)/2\pi$ then has the units

$(\text{Pa})^2/\text{Hz}$ or $(\text{psi})^2/\text{Hz}$ and the displacement covariance matrix, Equation (53), becomes

$$[W_{mn} W_{kl}] = \frac{1}{8} \sum_j \{\phi\}_j \frac{S_f}{\mu_j^2 \zeta_j \lambda_{oj} \lambda_j^2} \{\phi\}_j^T \quad (60)$$

where S_f is a nondimensional forcing spectral density parameter defined as

$$S_f = \frac{S_p(f)}{\rho^2 h^4 (D/\rho b^4)^{3/2}} \quad (61)$$

and

$$\omega^2 = \lambda_o^2 \left(\frac{D}{\rho h b^4} \right) \quad (62)$$

$$\Omega^2 = \lambda^2 \left(\frac{D}{\rho h b^4} \right) \quad (63)$$

$$\mu = M/\rho h^2 \quad (64)$$

The frequency parameters λ_o and λ , and the mass parameter μ are all dimensionless quantities. This nondimensional spectral density parameter of acoustic pressure excitation S_f will be used for the numerical results presented in the next section.

3. DEFLECTION AND STRAINS

From Equation (8), the mean-square deflection of the plate is given by

$$\overline{\left(\frac{w}{h}\right)^2} = \sum_m \sum_n \sum_k \sum_l \overline{w_{mn} w_{kl}} f_m(x) f_k(x) g_n(y) g_l(y) \quad (65)$$

where the averages $\overline{w_{mn} w_{kl}} = \xi[w_{mn} w_{kl}]$ have been determined in Equation (53). The mean-square center deflection can be obtained from Equation (65).

For a clamped rectangular plate ($a > b$), the maximum bending strain occurs at the extreme-fiber ($z = \pm h/2$) at the midpoint ($x = a/2$) of the long edge and perpendicular (ϵ_y) to the long edge. The bending strain at the extreme-fiber and in the y-direction is

$$\epsilon_{by} = \pm \frac{h}{2} \frac{\partial^2 w}{\partial y^2} \quad (66)$$

or

$$\begin{aligned} \frac{\epsilon_{by} b^2}{h^2} = & \pm \frac{\pi^2}{2} \sum_m \sum_n f_m(x) \left[(n-1)^2 \cos \frac{(n-1)\pi y}{b} \right. \\ & \left. - (n+1)^2 \cos \frac{(n+1)\pi y}{b} \right] w_{mn} \end{aligned} \quad (67)$$

The membrane strain in the y-direction, Equations (15, 20, 29 and 30), in terms of generalized displacements w_{mn} is

$$\begin{aligned} \frac{\epsilon_{oy} b^2}{h^2} = & \frac{\pi^2}{8} \sum_m \sum_n w_{mn} Z_y(w_{mn}) \\ & + \sum_m \sum_n \sum_k \sum_l \sum_p \sum_q C_{pq} B_{pqmnkl} w_{mn} w_{kl} \end{aligned} \quad (68)$$

where

$$C_{pq} = \frac{\pi^2 (v q^2 - p^2/a^2)}{(p^2/a + q^2/a)^2} \cos \frac{p\pi x}{a} \cos \frac{q\pi y}{b} \quad (69)$$

The total strain is then given by

$$\epsilon_y = \epsilon_{oy} + \epsilon_{by} \quad (70)$$

and the mean-square strain becomes

$$\overline{\epsilon_y^2} = \overline{\epsilon_{oy}^2} + 2\overline{\epsilon_{oy} \epsilon_{by}} + \overline{\epsilon_{by}^2} \quad (71)$$

For Gaussian random processes with zero-mean, the generalized displacements follow the relations

$$\xi[W_{ij} W_{kl} W_{mn}] = 0 \quad (72)$$

$$\begin{aligned} \xi[W_{ij} W_{kl} W_{mn} W_{rs}] &= \xi[W_{ij} W_{kl}] \xi[W_{mn} W_{rs}] \\ &+ \xi[W_{ij} W_{mn}] \xi[W_{kl} W_{rs}] + \xi[W_{ij} W_{rs}] \xi[W_{kl} W_{mn}] \end{aligned} \quad (73)$$

and the RMS maximum strain can be determined from Equation (71).

SECTION III

RESULTS AND DISCUSSION

1. GENERAL COMMENTS

Since the solution developed in Section II is of the infinite series type, it is important to understand its convergence behavior. The experience gained in Reference 20 on convergence of the solution for the large deflection under thermal loading aids in truncation of the series in a rational manner.

The convergence of the solution is examined through a study of square and rectangular panels subjected to a normal incidence acoustic impingement. Since the loading is symmetric, therefore, only symmetric generalized displacements are retained in the transverse deflection function. The particular generalized displacements that were chosen to be nonzero in the convergence study are shown in Table 1. Numerical results are provided for the mean-square plate center deflection and the mean-square maximum strain for a lateral deflection series that varies in size from four, six, ten and to fifteen terms. The maximum strain occurs at the extreme-fiber ($z = \pm h/2$) perpendicular to the long edge (ϵ_y) and at the midpoint ($x = a/2$). In the results presented, the white noise excitation is band-limited with a frequency bandwidth of 25 Hz to 6,000 Hz as shown in Figure 8, the damping ratio is assumed to be constant for all four normal modes and Poisson's ratio is equal to 0.33. The computer program is, however, much more flexible that the spectral density of pressure excitation could be varying slowly in the neighborhood of equivalent linear frequency Ω_j and also the damping ratios could be different for different normal coordinates.

TABLE 1. GENERALIZED DISPLACEMENTS FOR CONVERGENCE STUDIES.

Generalized Displacements	<u>Number of terms</u>			
	<u>4</u>	<u>6</u>	<u>10</u>	<u>15</u>
W_{11}	X	X	X	X
W_{13}	X	X	X	X
W_{31}	X	X	X	X
W_{33}	X	X	X	X
W_{15}		X	X	X
W_{51}		X	X	X
W_{35}			X	X
W_{53}			X	X
W_{17}			X	X
W_{71}			X	X
W_{55}				X
W_{37}				X
W_{73}				X
W_{19}				X
W_{91}				X

2. CONVERGENCE OF THE NONLINEAR RANDOM RESPONSE

The convergence of the solution technique was examined to determine the degree of accuracy possible with a highly truncated transverse deflection function series. The mean-square nondimensional center deflection versus the nondimensional spectral density parameter S_f using 4, 6, 10 and 15

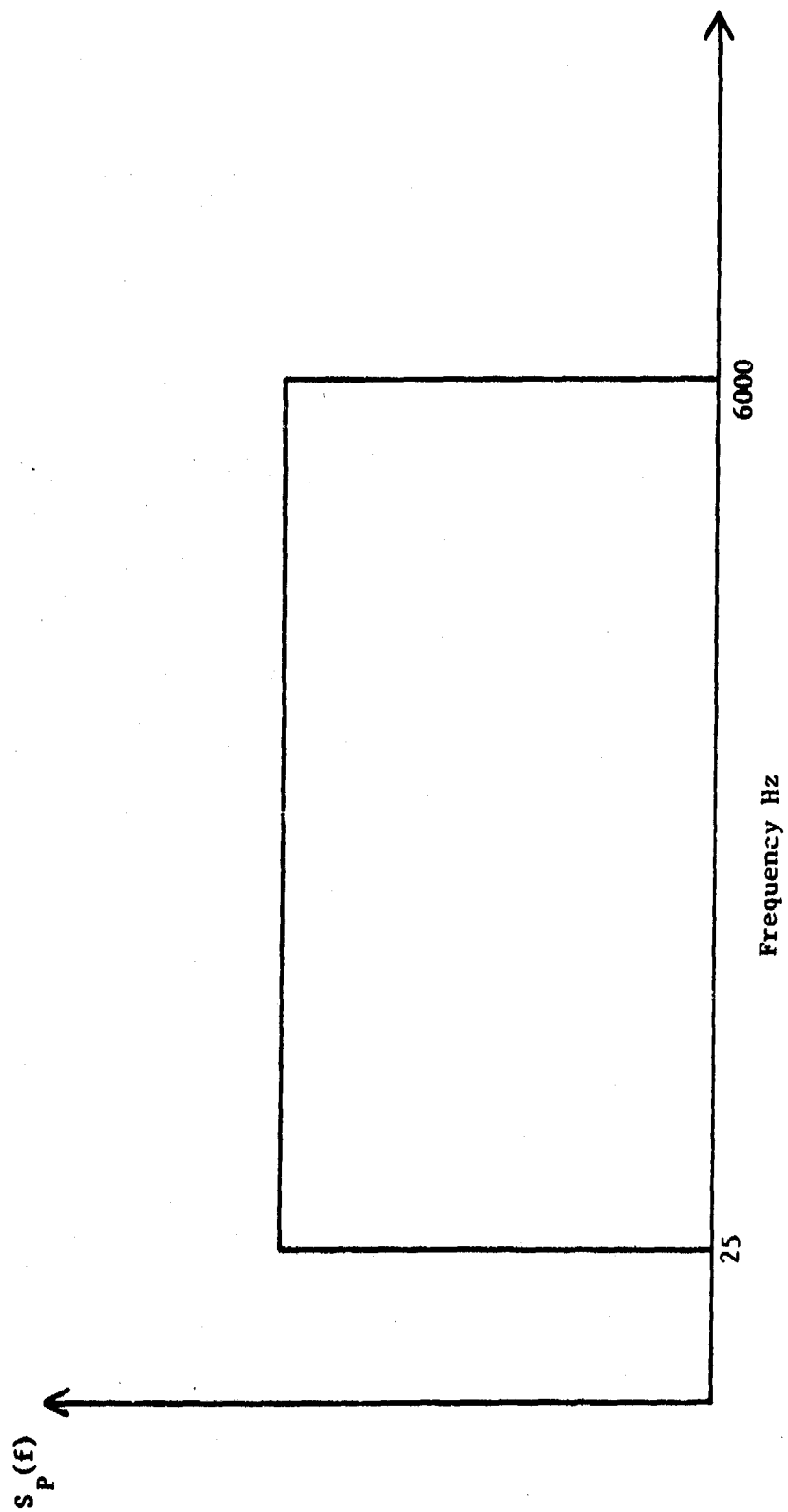


Figure 8. Band-Limited White Noise Excitation

terms in the deflection function for a square and a rectangular ($\alpha = 2$) plate are shown in Figures 9 and 10, respectively. It clearly indicates that a 6-term solution gives accurate results for the nonlinear maximum deflection while a 4-term solution will provide very accurate linear results. Figures 11 and 12 show the maximum mean-square strain versus the nondimensional pressure spectral density for the square and rectangular ($\alpha = 2$) plates, respectively, using 4, 6, 10 and 15 terms in the deflection function. It can be seen that the convergence of the mean-square strain is much slower as compared with that of the mean-square deflection. More number of terms, therefore, are needed in the deflection function for accurate determination of strains. Results of maximum mean-square strain based on small deflection linear theory are also given in the figures. The use of linear theory would lead to poor estimation of panel fatigue life.

3. EFFECTS OF PANEL DAMPING

Figures 13 and 14 show the mean-square nondimensional center deflection versus the nondimensional spectral density of acoustic pressure excitation for rectangular panels of length-to-width ratio $\alpha = 1$ and 2 with the damping ratio equal to 0.009, 0.018 and 0.027. Figures 15 and 16 show the maximum mean-square nondimensional strain versus the nondimensional pressure spectral density for rectangular plates of aspect ratios of 1 and 2 with different panel damping ratios. Ten terms were included in the deflection function to generate those results shown in Figures 13 through 16. It is clear from the figures that the precise determination of panel damping is very important.

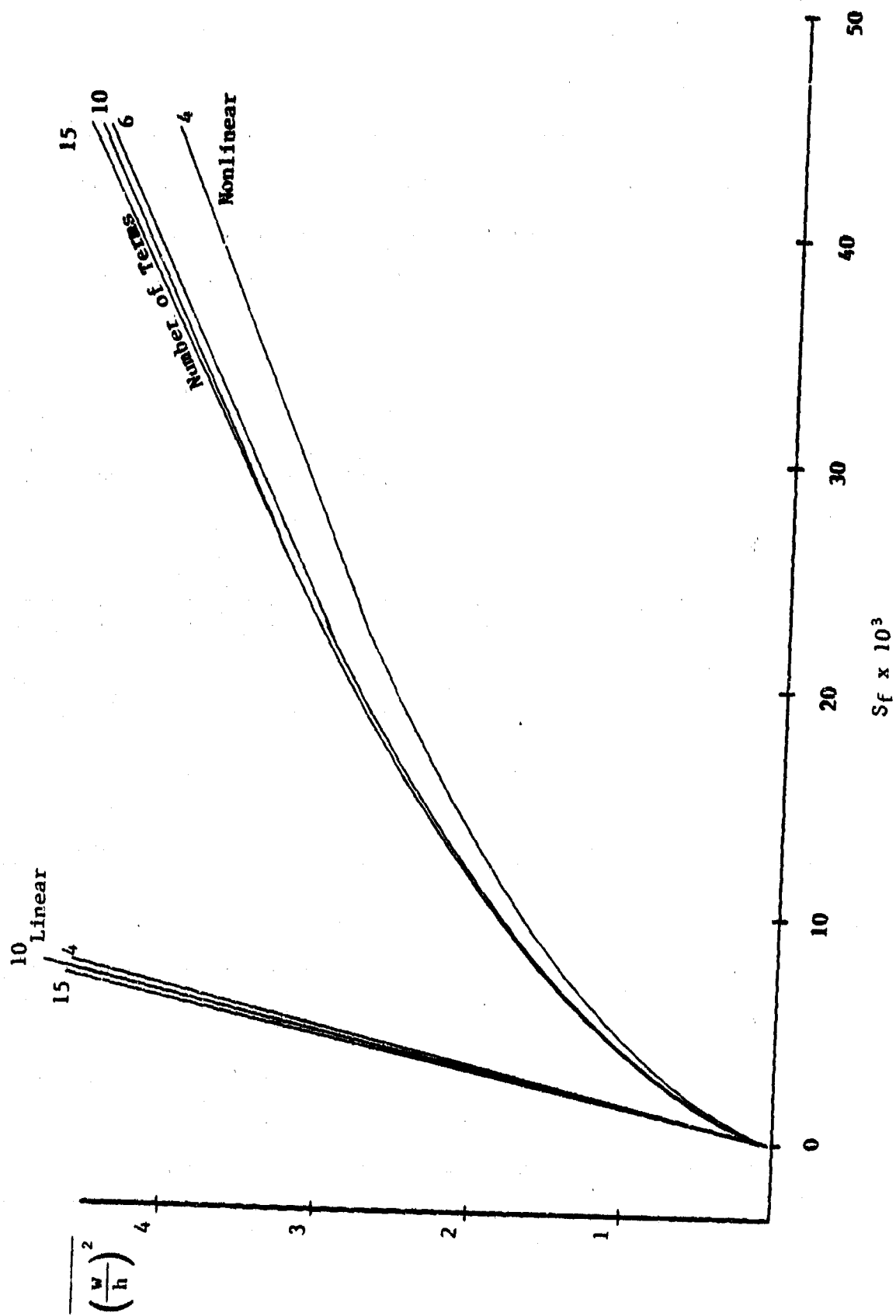


Figure 9. Convergence of the Mean-Square Center Deflection for the Square Plate ($\nu=0.009$)

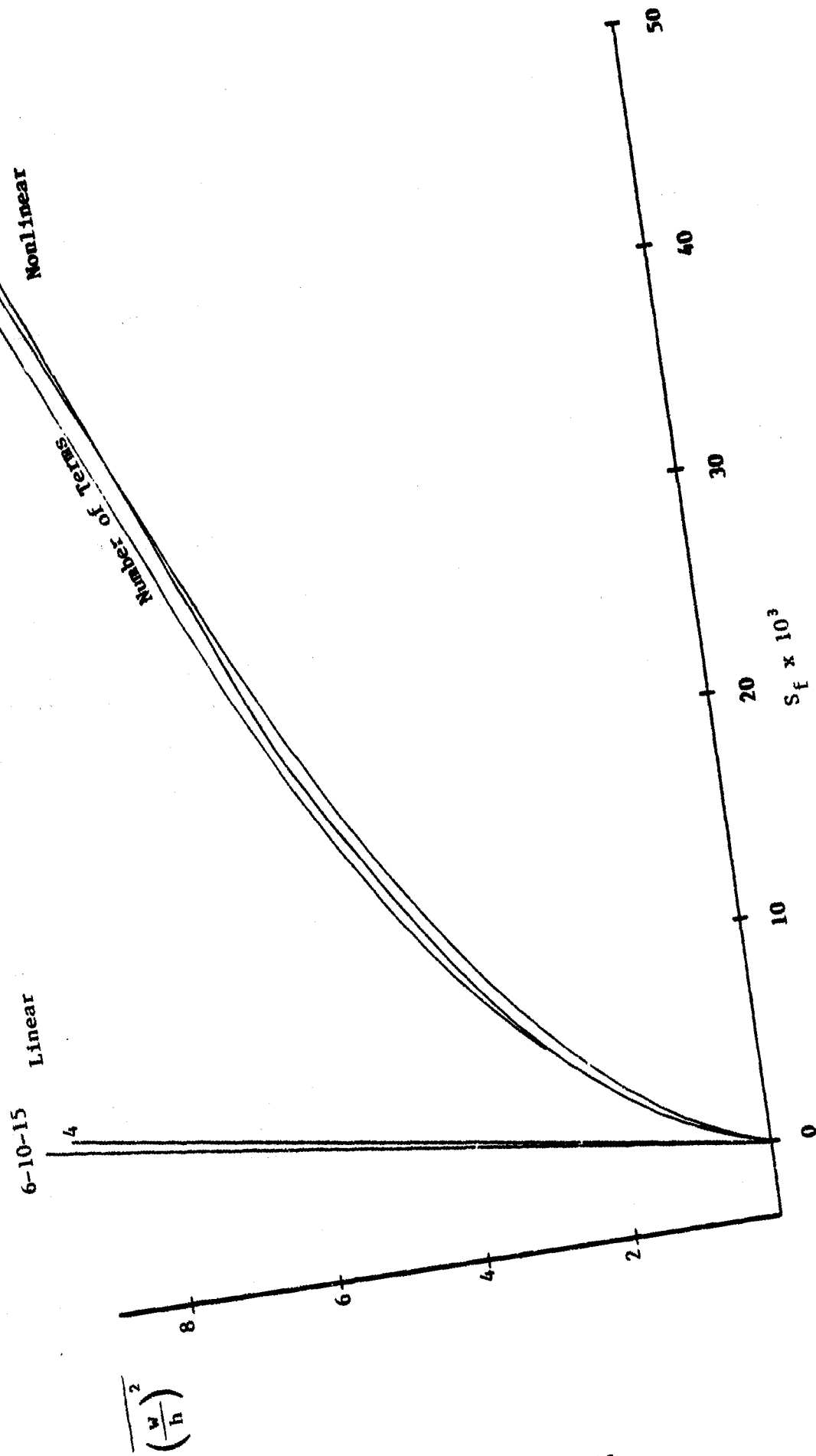


Figure 10. Convergence of the Mean-Square Center Deflection for the Rectangular ($\nu=2$) Plate ($\tau=0.009$)

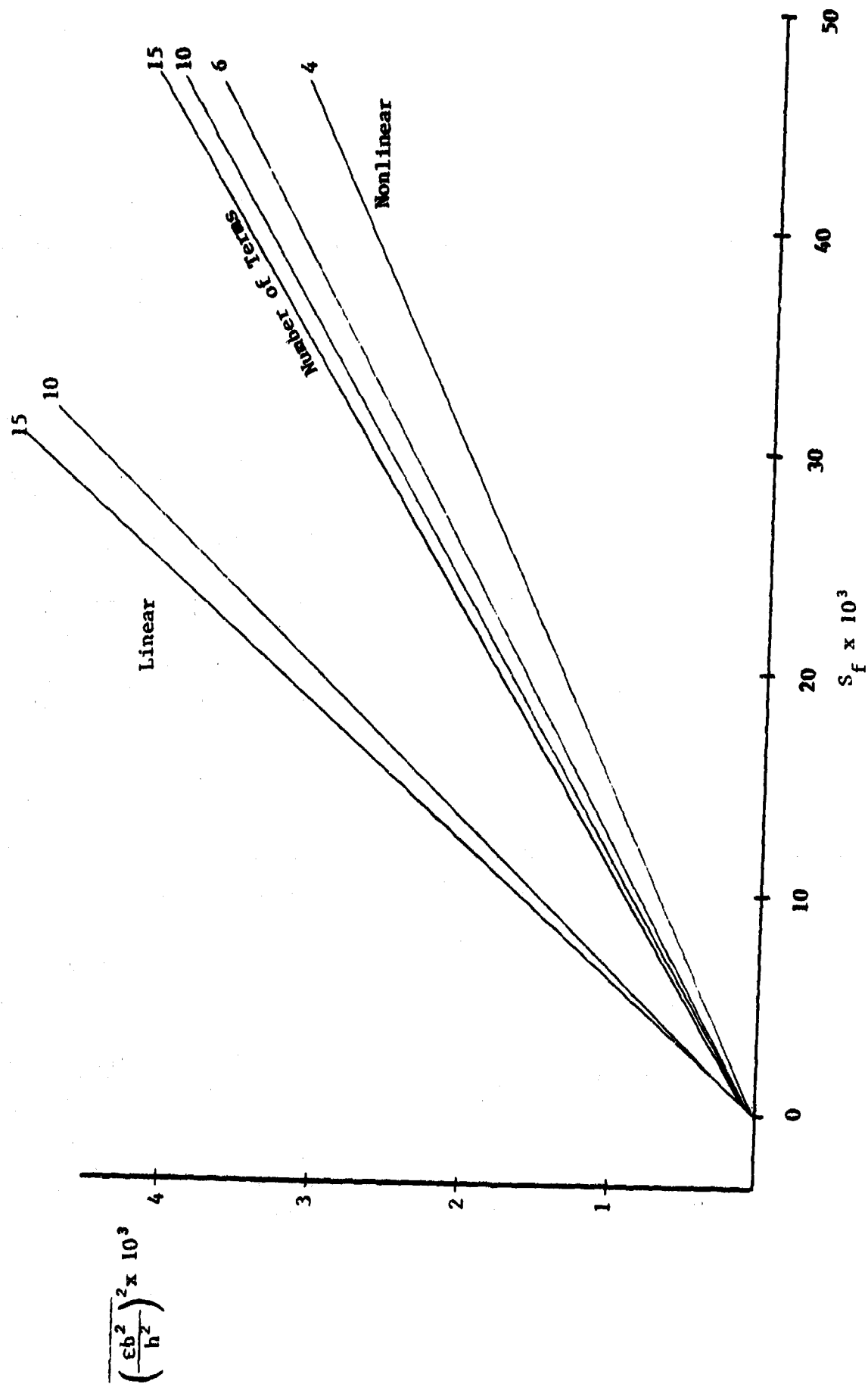


Figure 11. Convergence of the Maximum Mean-Square Strain for the Square Plate ($\nu=0.009$)

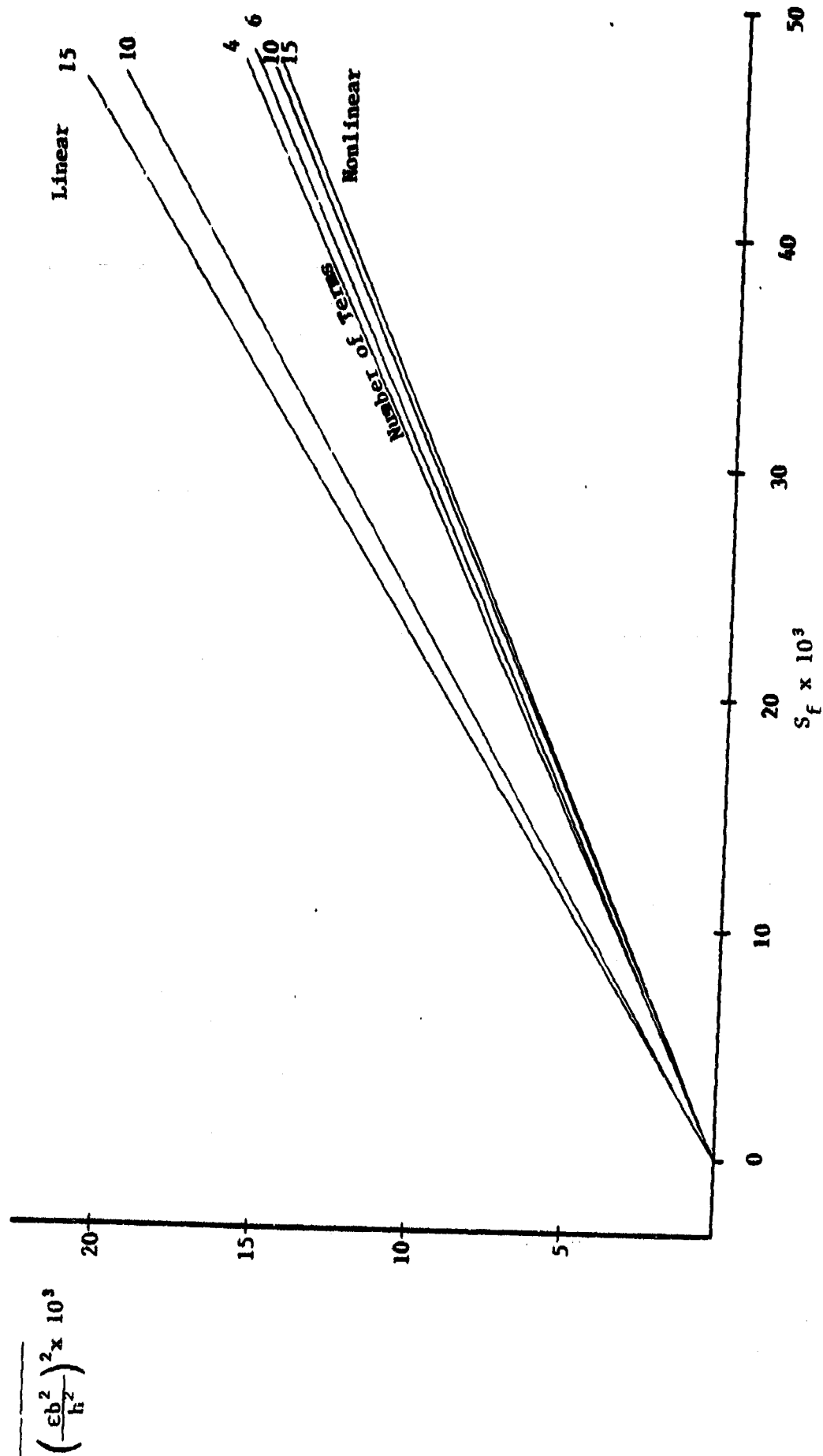


Figure 12. Convergence of the Maximum Mean-Square Strain for the Rectangular ($\alpha=2$) Plate ($\zeta=0.009$)

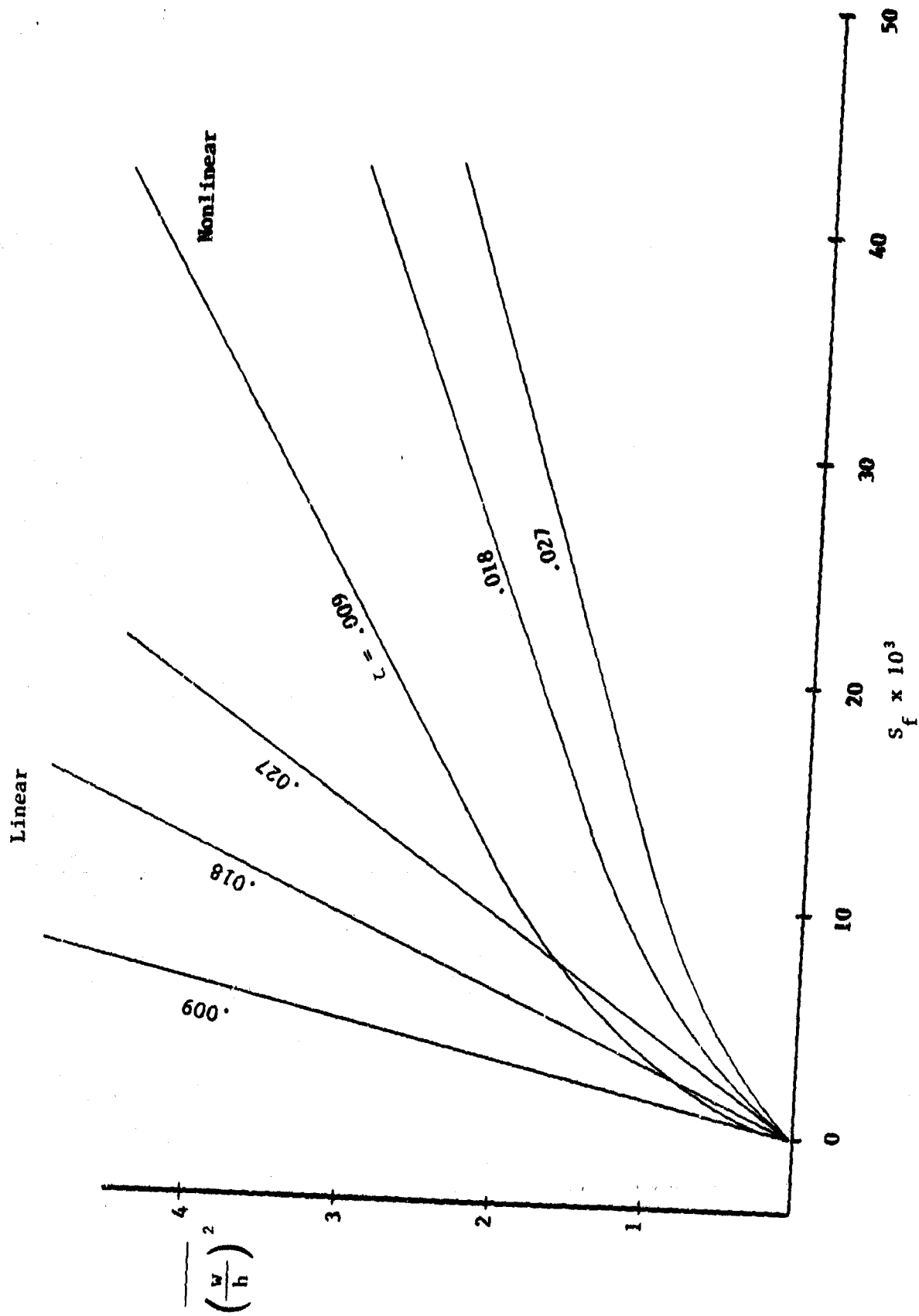


Figure 13. Effects of Damping on Mean-Square Center Deflection for a Clamped Square Plate

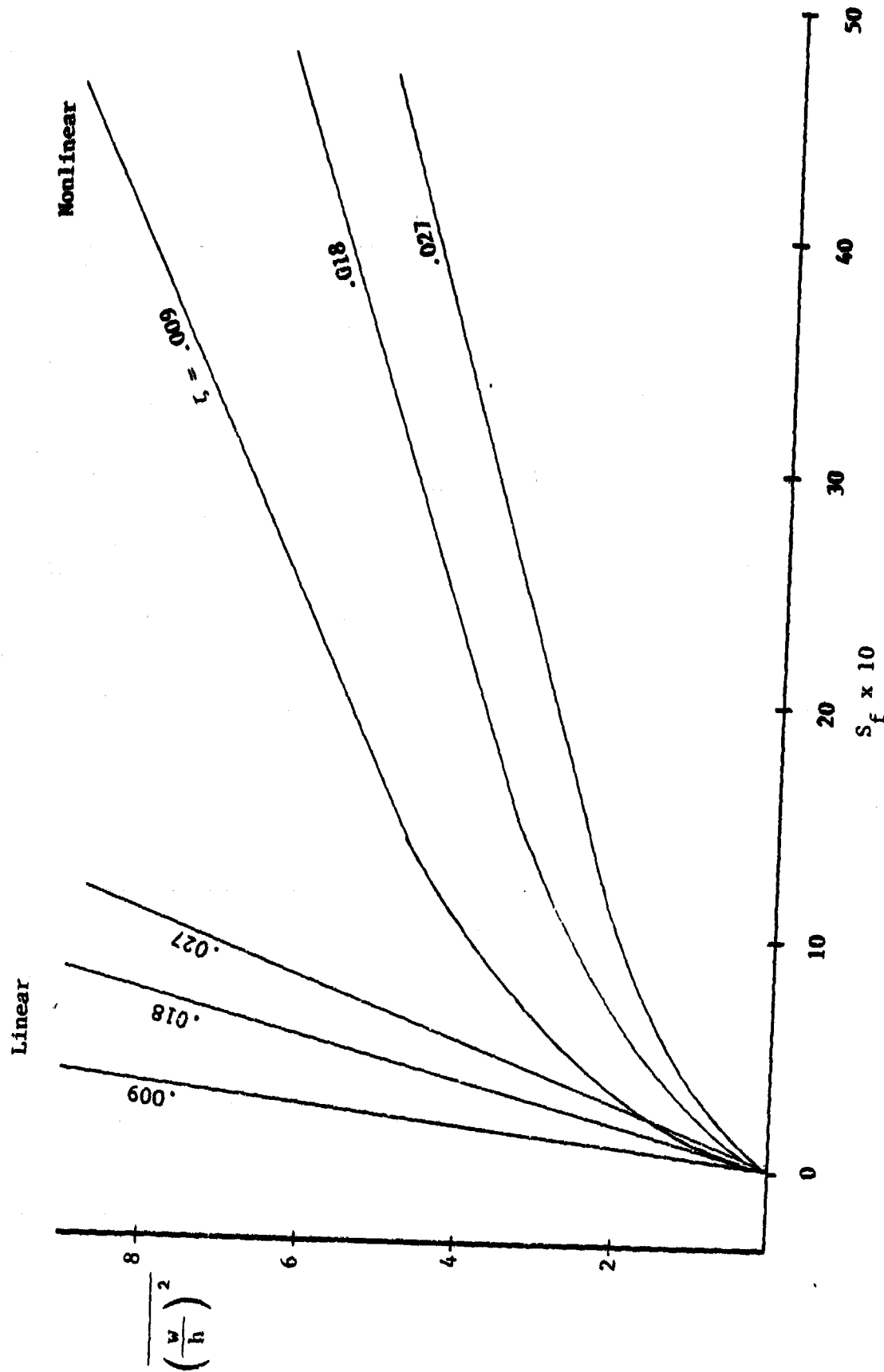


Figure 14. Effects of Damping on Mean-Square Center Deflection for a Clamped Rectangular Plate ($\alpha = 2$)

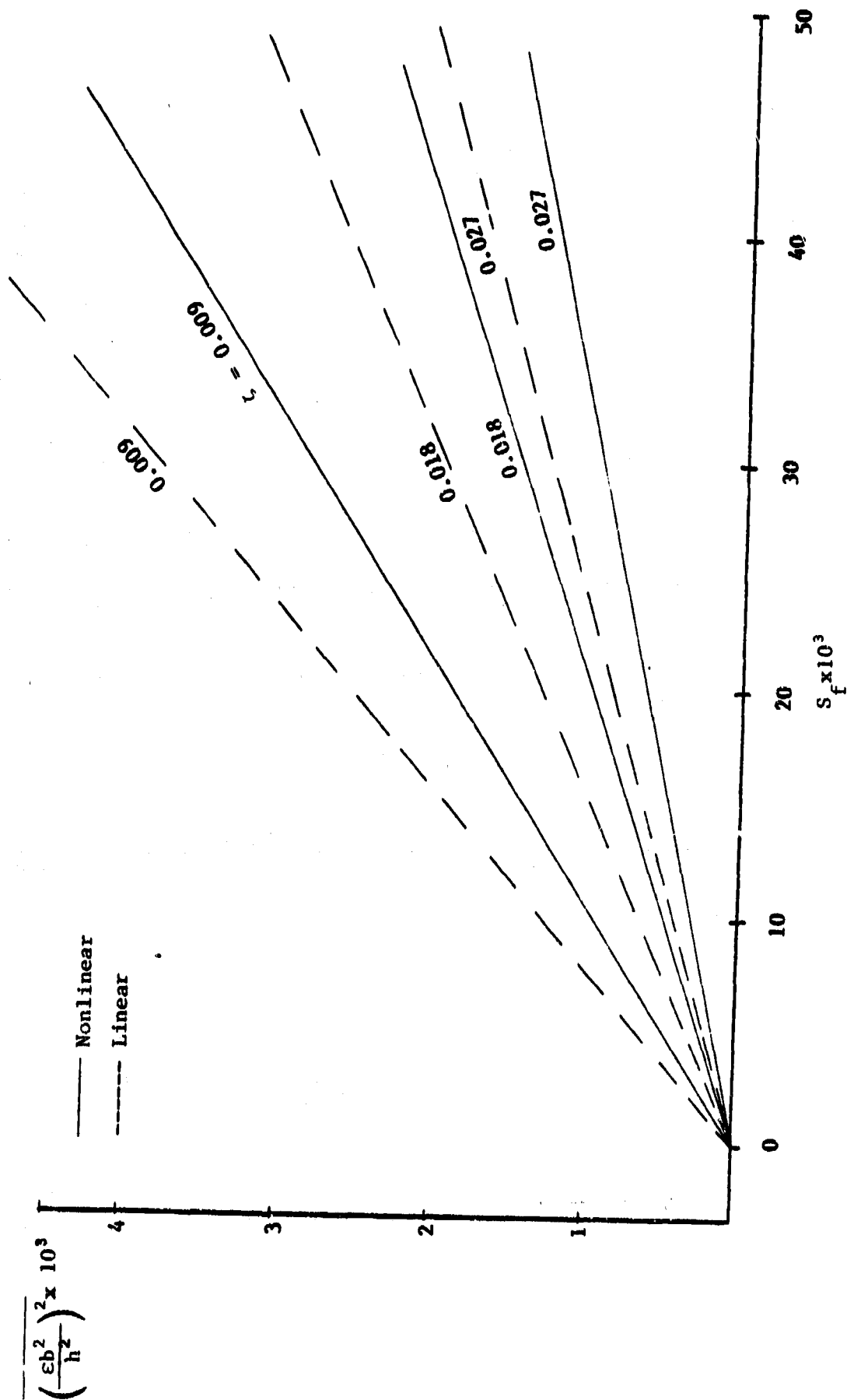


Figure 15. Effects of Damping on Maximum Mean-Square Strain for a Clamped Square Plate

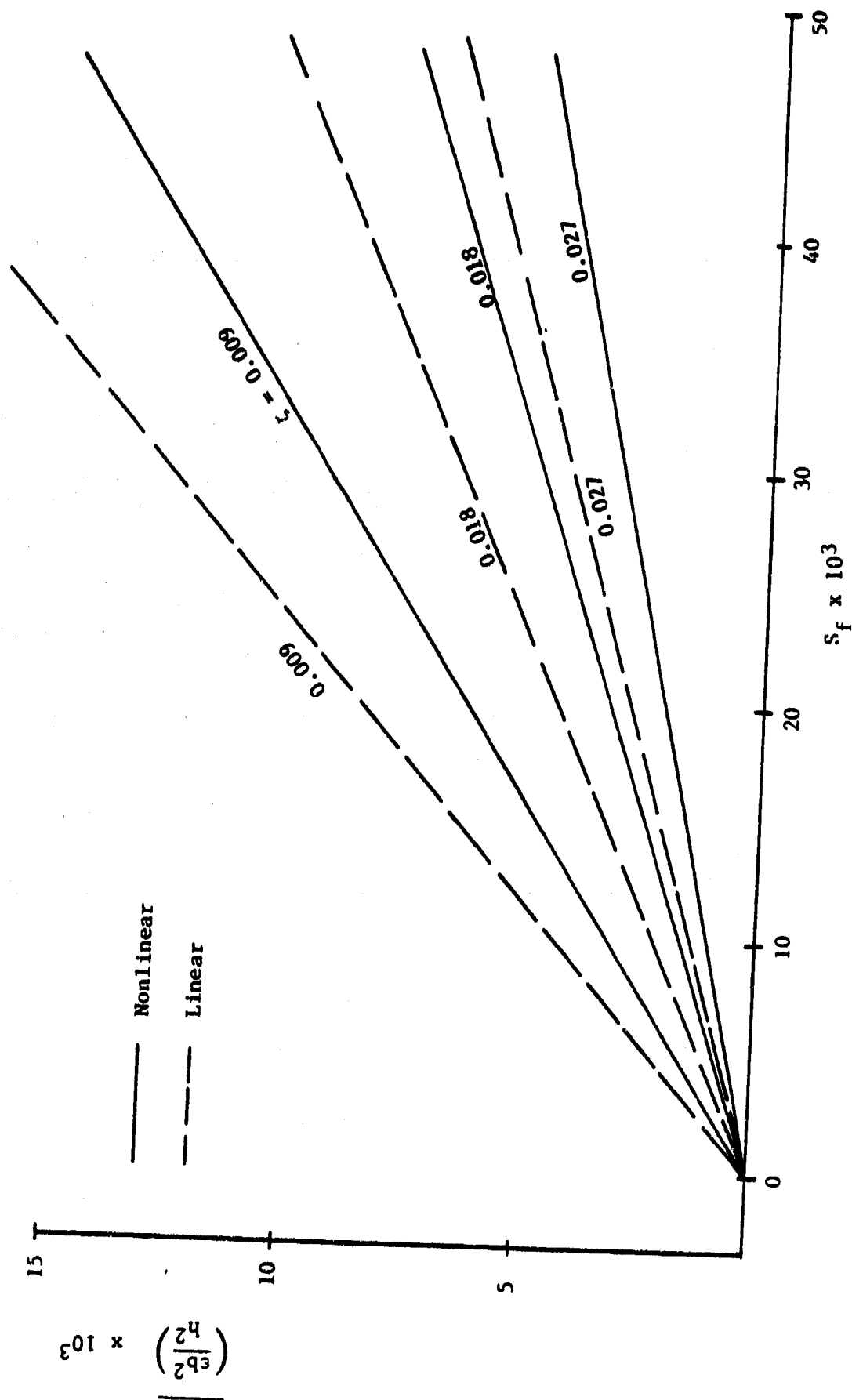


Figure 16. Effects of Damping on Maximum Mean-Square Strain for a Clamped Rectangular ($\alpha = 2$) Plate.

SECTION IV

CONCLUDING REMARKS

A "quasi-exact" analytical procedure was developed for the prediction of the nonlinear random response of rigidly clamped rectangular panels subjected to broadband noise excitation. Multiple (4) modes were employed in the formulation. A computer program has been developed to aid in the determination of RMS center deflection, RMS maximum strain and equivalent linear frequency at given pressure spectral density of excitation.

The convergence of the present analytical method was demonstrated through a detailed study of a square and a rectangular ($\alpha = 2$) plate under normal incidence acoustic impingements. Results were presented for both panels with the truncated lateral deflection function series of 4, 6, 10 and 15 terms. This study revealed that convergence is very rapid for the determination of central deflection, but much slower in the prediction of strains. Accurate mean-square deflections can be obtained with the use of six terms in the deflection function, while it is necessary to consider as many as 10 or more terms for the accurate determination of the strains. This computed RMS strain and equivalent linear frequency, in conjunction with strain versus cycles to failure (S-N) data, should be used for the estimation of service life.

In the numerical examples presented, a constant damping ratio was used for all excitation levels. The total damping includes the acoustic radiation damping, panel edge damping and the material damping in the panel itself. Nonlinear damping phenomena, however, have been observed in experiments. Strain response data for an aluminum panel of 3.94 cm x 3.94 cm x 0.25 mm at three different overall sound pressure levels (130, 142 and 160

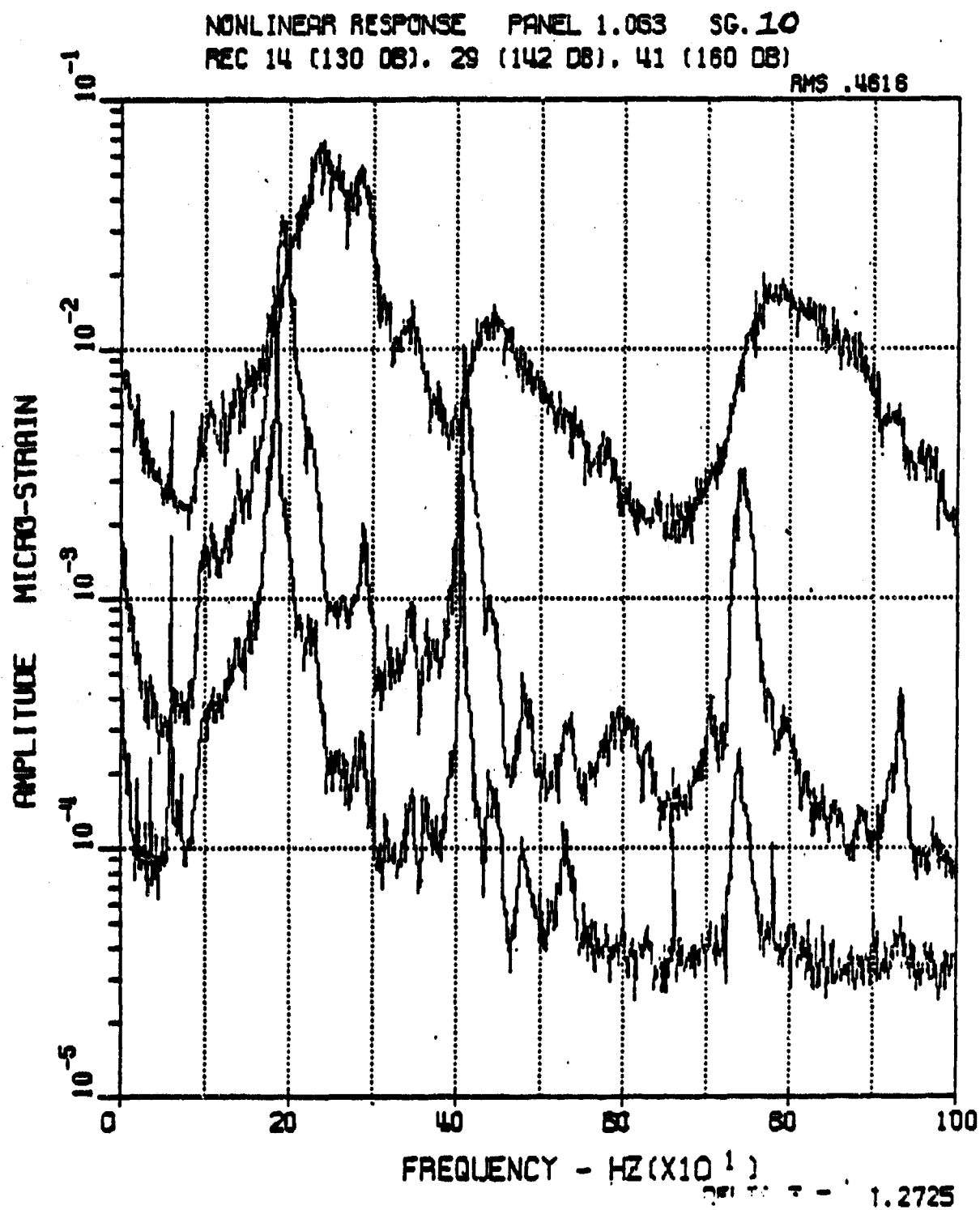


Figure 17. Strain Response of a Square Aluminum Panel
at Three Different Sound Pressure Levels

dB) obtained in Reference 12 are shown in Figure 17. At the low-excitation levels, the modal responses of the panel can be clearly seen. At the highest level, broadening of the response peak due to nonlinear damping is observed. Therefore, more effort is needed to better understand the effects of nonlinear damping on panel response.

APPENDIX A

INTEGRALS OF $\int_0^b \int_0^a L(w, F) f_r g_s dx dy$

$$\int_0^b \int_0^a D \frac{\partial^4 w}{\partial x^4} f_r g_s dx dy = \frac{Dh\pi^4 ab}{4a^4}$$

$$\begin{aligned} & \cdot \{[(r-1)^4 + (r+1)^4] [(C_1 + 1)W_{r,s} - W_{r,s-2} - W_{r,s+2}] \\ & + (r-1)^4 [W_{r-2,s-2} + W_{r-2,s+2} - (C_1 + 1)W_{r-2,s}] \\ & + (r+1)^4 [W_{r+2,s+2} + W_{r+2,s-2} - (C_1 + 1)W_{r+2,s}]\} \end{aligned} \quad (A1)$$

$$\int_0^b \int_0^a D \frac{\partial^4 w}{\partial y^4} f_r g_s dx dy = \frac{Dh\pi^4 ab}{4b^4}$$

$$\begin{aligned} & \cdot \{[(s-1)^4 + (s+1)^4] [(C_2 + 1)W_{r,s} - W_{r-2,s} - W_{r+2,s}] \\ & + (s-1)^4 [W_{r-2,s-2} + W_{r+2,s-2} - (C_2 + 1)W_{r,s-2}] \\ & + (s+1)^4 [W_{r+2,s+2} + W_{r-2,s+2} - (C_2 + 1)W_{r,s+2}]\} \end{aligned} \quad (A2)$$

$$\int_0^b \int_0^a 2D \frac{\partial^4 w}{\partial x^2 \partial y^2} f_r g_s dx dy = \frac{Dh\pi^4 ab}{a^2 b^2}$$

$$\begin{aligned} & \cdot \{(r-1)^2 (s+1)^2 [W_{r,s} - W_{r,s+2} - W_{r+2,s} + W_{r+2,s+2}] \\ & + (r-1)^2 (s+1)^2 [W_{r,s} - W_{r,s+2} - W_{r-2,s} + W_{r-2,s+2}] \end{aligned}$$

$$\begin{aligned}
& + (r+1)^2 (s-1)^2 [W_{r,s} - W_{r,s-2} - W_{r+2,s} + W_{r+2,s-2}] \\
& + (r-1)^2 (s-1)^2 [W_{r,s} - W_{r,s-2} - W_{r-2,s} + W_{r-2,s-2}] \} \quad (A3)
\end{aligned}$$

$$\begin{aligned}
\int_0^b \int_0^a \rho h \frac{\partial^2 w}{\partial t^2} f_r g_s dx dy &= \frac{\rho h^2 ab}{4} \\
& \cdot [(C_3 + 2)(C_4 + 2)W_{r,s} - (C_3 + 2)W_{r+2,s} - (C_3 + 2)(C_4 + 1)W_{r-2,s} \\
& - (C_4 + 2)W_{r,s+2} - (C_3 + 1)(C_4 + 2)W_{r,s-2} + W_{r+2,s+2} \\
& + (C_3 + 1)W_{r+2,s-2} + (C_4 + 1)W_{r-2,s+2} + (C_3 + 1)(C_4 + 1)W_{r-2,s-2}] \quad (A4)
\end{aligned}$$

$$\begin{aligned}
\iint p(t) f_r g_s dx dy &= ab p(t) \quad \text{when } r = s = 1 \\
&= 0 \quad \text{otherwise} \quad (A5)
\end{aligned}$$

$$\begin{aligned}
-h \int_0^b \int_0^a F_{,yy} w_{,xx} f_r g_s dx dy &= ab [(\beta_{rs})_1 + (\beta_{rs})_2] = \\
& \left[\begin{aligned} (m+1)^2 & \left[\begin{aligned} & 2(n+s)^2 A_1(n+s) - (n+s-2)^2 A_1(n+s-2) - \\ & (n+s+2)^2 A_1(n+s+2) - 2(n-s)^2 A_1(n-s) + \\ & (n-s+2)^2 A_1(n-s+2) + (n-s-2)^2 A_1(n-s-2) \end{aligned} \right] \\ + (m-1)^2 & \left[\begin{aligned} & 2(n+s)^2 A_2(n+s) - (n+s-2)^2 A_2(n+s-2) - \\ & (n+s+2)^2 A_2(n+s+2) - 2(n-s)^2 A_2(n-s) + \\ & (n-s+2)^2 A_2(n-s+2) + (n-s-2)^2 A_2(n-s-2) \end{aligned} \right] \end{aligned} \right] \\
& + \frac{Eh^4 \pi^4}{16 ab} \sum_{m=1}^{\infty} W_{mn} \\
& + \frac{P_x h^2 \pi^2 b}{4a} \left[\begin{aligned} & [(r+1)^2 + (r-1)^2] \cdot [W_{r,s+2} + W_{r,s-2} - (C_1+1)W_{r,s}] + \\ & (r+1)^2 [C_1+1]W_{r+2,s} - W_{r+2,s+2} - W_{r+2,s-2} + \\ & (r-1)^2 [(C_1+1)W_{r-2,s} - W_{r-2,s-2} - W_{r-2,s+2}] \end{aligned} \right] \quad (A6)
\end{aligned}$$

$$-h \int_0^b \int_0^a F_{,xx} w_{,yy} f_r g_s dx dy = ab[(\beta_{rs})_3 + (\beta_{rs})_4] =$$

$$\begin{aligned} & \frac{Eh^4 \pi^4}{16 ab} \sum_{n=1}^{\infty} W_{mn} \\ & + \frac{p_y h^2 \pi^2 a}{4b} \left[\begin{aligned} & (n+1)^2 \left[\begin{aligned} & 2(m+r)^2 A_3(m+r) - (m+r-2)^2 A_3(m+r-2) - \\ & (m+r+2)^2 A_3(m+r+2) - 2(m-r)^2 A_3(m-r) + \\ & (m-r+2)^2 A_3(m-r+2) + (m-r-2)^2 A_3(m-r-2) \end{aligned} \right] \\ & + (n-1)^2 \left[\begin{aligned} & 2(m+r)^2 A_4(m+r) - (m+r-2)^2 A_4(m+r-2) - \\ & (m+r+2)^2 A_4(m+r+2) - 2(m-r)^2 A_4(m-r) + \\ & (m-r+2)^2 A_4(m-r+2) + (m-r-2)^2 A_4(m-r-2) \end{aligned} \right] \\ & + [(s+1)^2 + (s-1)^2] \cdot [W_{r+2,s} + W_{r-2,s} - (C_2+1)W_{r,s}] \\ & + (s+1)^2 [(C_2+1)W_{r,s+2} - W_{r-2,s} - W_{r+2,s+2}] + \\ & (s-1)^2 [(C_2+1)W_{r,s-2} - W_{r-2,s-2} - W_{r+2,s-2}] \end{aligned} \right] \quad (A7) \end{aligned}$$

$$2h \int_0^b \int_0^a F_{,xy} w_{,xy} f_r g_s dx dy = ab(\beta_{rs})_5 =$$

$$\begin{aligned} & \frac{Eh^4 \pi^4}{8 ab} \sum_{n=1}^{\infty} W_{mn} \\ & \left[\begin{aligned} & (m-1)(n-1)[(m+r) A_5(m+r) - |m-r| A_5(m-r) - \\ & (m+r-2) A_5(m+r-2) + |m-r-2| A_5(m-r-2)] + \\ & (m-1)(n+1)[(m+r) A_6(m+r) - |m-r| A_6(m-r) - \\ & (m+r-2) A_6(m+r-2) + |m-r-2| A_6(m-r-2)] + \\ & (m+1)(n-1)[(m+r) A_5(m+r) - |m-r| A_5(m-r) - \\ & (m+r+2) A_5(m+r+2) + |m-r+2| A_5(m-r+2)] + \\ & (m+1)(n+1)[(m+r) A_6(m+r) - |m-r| A_6(m-r) - \\ & (m+r+2) A_6(m+r+2) + |m-r+2| A_6(m-r+2)] \end{aligned} \right] \quad (A8) \end{aligned}$$

where; $W_{ij} = 0$ for i or $j < 1$; $F_{\pm p, \pm q} = F_{p, q}$;

$$A_1(k) = C(m+r+2)F_{m+r+2,k} + C(m-r)F_{m-r,k} - C(m+r)F_{m+r,k} - C(m-r+2)F_{m-r+2,k}$$

$$A_2(k) = C(m+r-2)F_{m+r-2,k} + C(m-r)F_{m-r,k} - C(m+r)F_{m+r,k} - C(m-r-2)F_{m-r-2,k}$$

$$A_3(k) = C(n+s+2)F_{k,n+s+2} + C(n-s)F_{k,n-s} - C(n+s)F_{k,n+s} - C(n-s+2)F_{k,n-s+2}$$

$$A_4(k) = C(n+s-2)F_{k,n+s-2} + C(n-s)F_{k,n-s} - C(n+s)F_{k,n+s} - C(n-s-2)F_{k,n-s-2}$$

$$A_5(k) = (n+s)F_{k,n+s} + |n-s-2|F_{k,n-s-2} - (n+s-2)F_{k,n+s-2} - |n-s|F_{k,n-s}$$

$$A_6(k) = (n+s)F_{k,n+s} + |n-s+2|F_{k,n-s+2} - (n+s+2)F_{k,n+s+2} - |n-s|F_{k,n-s}$$

and;

$$C(k) = \begin{cases} 2 & \text{for } k = 0 \\ 1 & \text{for } k \neq 0 \end{cases} \quad C_1 = \begin{cases} 2 & \text{for } s = 1 \\ 1 & \text{for } s \neq 1 \end{cases} \quad C_2 = \begin{cases} 2 & \text{for } r = 1 \\ 1 & \text{for } r \neq 1 \end{cases}$$

$$C_3 = \begin{cases} 1 & \text{for } s = 1 \\ 0 & \text{for } s \neq 1 \end{cases} \quad C_4 = \begin{cases} 1 & \text{for } r = 1 \\ 0 & \text{for } r \neq 1 \end{cases} \quad (A10)$$

APPENDIX B

GENERALIZED EQUIVALENT LINEAR STIFFNESS MATRIX $[K]_{EL}$

The elements of the equivalent linear stiffness matrix are derived from the expression

$$K_{rsij} = \xi \left[\frac{\partial \beta_{rs}}{\partial w_{ij}} \right] \quad (B1)$$

The function β_{rs} is associated with the integrals after applying the Bubnov-Galerkin approach to the equation of motion in deflection, and it can be expressed as the sum of five subfunctions as

$$\begin{aligned} \beta_{rs} &= -\frac{h}{ab} \int_0^b \int_0^a (F_{,yy} w_{,xx} + F_{,xx} w_{,yy} - 2F_{,xy} w_{,xy}) f_r g_s dx dy \\ &= (\beta_{rs})_1 + (\beta_{rs})_2 + (\beta_{rs})_3 + (\beta_{rs})_5 \end{aligned} \quad (B2)$$

The equivalent linear stiffness matrix will consist of five submatrices

as

$$[K]_{ZL} = [K]_1 + [K]_2 + [K]_3 + [K]_4 + [K]_5 \quad (B3)$$

The elements of the submatrices are given as the following

$$(K_{rsij})_1 =$$

$$\begin{aligned} & \frac{Eh^4\pi^4}{16a^2b^2} \{ (i+1)^2 [2(j+s)^2 A_1(j+s) - (j+s-2)^2 A_1(j+s-2) \\ & \quad - (j+s+2)^2 A_1(j+s+2) - 2(j-s)^2 A_1(j-s) \\ & \quad + (j-s+2)^2 A_1(j-s+2) + (j-s-2)^2 A_1(j-s-2)] \\ & + (i-1)^2 [2(j+s)^2 A_2(j+s) - (j+s-2)^2 A_2(j+s-2) \\ & \quad - (j+s+2)^2 A_2(j+s+2) - 2(j-s)^2 A_2(j-s) \\ & \quad + (j-s+2)^2 A_2(j-s+2) + (j-s-2)^2 A_2(j-s-2)] \\ & + \sum_m \sum_n \{ (m+1)^2 [2(n+s)^2 A'_1(n+s) - (n+s-2)^2 A'_1(n+s-2) \\ & \quad - (n+s+2)^2 A'_1(n+s+2) - 2(n-s)^2 A'_1(n-s) \\ & \quad + (n-s+2)^2 A'_1(n-s+2) + (n-s-2)^2 A'_1(n-s-2)] \\ & + (m-1)^2 [2(n+s)^2 A'_2(n+s) - (n+s-2)^2 A'_2(n+s-2) \\ & \quad - (n+s+2)^2 A'_2(n+s+2) - 2(n-s)^2 A'_2(n-s) \\ & \quad + (n-s+2)^2 A'_2(n-s+2) + (n-s-2)^2 A'_2(n-s-2)] \} \} \end{aligned}$$

$$\begin{aligned} (K_{rsij})_2 &= - \frac{Eh^2\pi^2}{4a^2(1-v^2)} \left\{ \left(\frac{v}{b} \xi[I_y(w_{mn})] + \frac{1}{a} \xi[I_x(w_{mn})] \right) \frac{\partial u(w_{rs})}{\partial w_{ij}} \right. \\ & \quad + \frac{h^2\pi^2}{4} \left(\frac{v}{b^2} \xi[Z_y(w_{ij}) u(w_{rs})] \right. \\ & \quad \left. \left. + \frac{1}{a^2} \xi[Z_x(w_{ij}) u(w_{rs})] \right) \right\} \quad (B5) \end{aligned}$$

$$\begin{aligned}
(K_{rsij})_4 = & - \frac{Eh^2\pi^2}{4b^2(1-\nu^2)} \left\{ \left(\frac{\nu}{a} \xi[I_x(W_{mn})] + \frac{1}{b} \xi[I_y(W_{mn})] \right) \frac{\partial v(W_{rs})}{\partial W_{ij}} \right. \\
& + \frac{h^2\pi^2}{4} \left(\frac{\nu}{a^2} \xi[Z_x(W_{ij}) v(W_{rs})] \right. \\
& \left. \left. + \frac{1}{b^2} \xi[Z_y(W_{ij}) v(W_{rs})] \right) \right\} \quad (B6)
\end{aligned}$$

$$\begin{aligned}
(K_{rsij})_5 = & \frac{Eh^4\pi^4}{8a^2b^2} \left\{ (i-1)(j-1) [(i+r)A_5(i+r) - |i-r|A_5(i-r) \right. \\
& \quad - (i+r-2)A_5(i+r-2) + |i-r-2|A_5(i-r-2)] \\
& \quad + (i-1)(j+1) [(i+r)A_6(i+r) - |i-r|A_6(i-r) \\
& \quad \quad - (i+r-2)A_6(i+r-2) + |i-r-2|A_6(i-r-2)] \\
& \quad + (i+1)(j-1) [(i+r)A_5(i+r) - |i-r|A_5(i-r) \\
& \quad \quad - (i+r+2)A_5(i+r+2) + |i-r+2|A_5(i-r+2)] \\
& \quad + (i+1)(j+1) [(i+r)A_6(i+r) - |i-r|A_6(i-r) \\
& \quad \quad - (i+r+2)A_6(i+r+2) + |i-r+2|A_6(i-r+2)] \\
& + \sum_m \sum_n \left\{ (m-1)(n-1) [(m+r)A'_5(m+r) - |m-r|A'_5(m-r) \right. \\
& \quad \quad - (m+r-2)A'_5(m+r-2) + |m-r-2|A'_5(m-r-2)] \\
& \quad + (m-1)(n+1) [(m+r)A'_6(m+r) - |m-r|A'_6(m-r) \\
& \quad \quad - (m+r-2)A'_6(m+r-2) + |m-r-2|A'_6(m-r-2)] \\
& \quad + (m+1)(n-1) [(m+r)A'_5(m+r) - |m-r|A'_5(m-r) \\
& \quad \quad - (m+r+2)A'_5(m+r+2) + |m-r+2|A'_5(m-r+2)] \\
& \quad + (m+1)(n+1) [(m+r)A'_6(m+r) - |m-r|A'_6(m-r) \\
& \quad \quad - (m+r+2)A'_6(m+r+2) + |m-r+2|A'_6(m-r+2)] \left. \right\} \left. \right\}
\end{aligned}$$

where

$$\begin{aligned}
 u(W_{rs}) = & [(r+1)^2 + (r-1)^2] [W_{r,s+2} + W_{r,s-2} - (C_1+1) W_{rs}] \\
 & + (r+1)^2 [(C_1+1) W_{r+2,s} - W_{r+2,s+2} - W_{r+2,s-2}] \\
 & + (r-1)^2 [(C_1+1) W_{r-2,s} - W_{r-2,s-2} - W_{r-2,s+2}] \quad (B8)
 \end{aligned}$$

$$\begin{aligned}
 v(W_{rs}) = & [(s+1)^2 + (s-1)^2] [W_{r+2,s} + W_{r-2,s} - (C_2+1) W_{rs}] \\
 & + (s+1)^2 [(C_2+1) W_{r,s+2} - W_{r-2,s+2} - W_{r+2,s+2}] \\
 & + (s-1)^2 [(C_2+1) W_{r,s-2} - W_{r-2,s-2} - W_{r+2,s-2}] \quad (B9)
 \end{aligned}$$

$$\begin{aligned}
 A_1(d) = & C(i+r+2)(F_\xi)_{i+r+2,d} + C(i-r)(F_\xi)_{i-r,d} \\
 & - C(i+r)(F_\xi)_{i+r,d} - C(i-r+2)(F_\xi)_{i-r+2,d} \quad (B10)
 \end{aligned}$$

$$\begin{aligned}
 A_2(d) = & C(i+r-2)(F_\xi)_{i+r-2,d} - C(i-r)(F_\xi)_{i-r,d} \\
 & - C(i+r)(F_\xi)_{i+r,d} - C(i-r-2)(F_\xi)_{i-r-2,d} \quad (B11)
 \end{aligned}$$

$$\begin{aligned}
 A_3(d) = & (j+s)(F_\xi)_{d,j+s} + |j-s-2|(F_\xi)_{d,j-s-2} \\
 & - (j+s-2)(F_\xi)_{d,j+s-2} - |j-s|(F_\xi)_{d,j-s} \quad (B12)
 \end{aligned}$$

$$\begin{aligned}
 A_4(d) = & (j+s)(F_\xi)_{d,j+s} + |j-s+2|(F_\xi)_{d,j-s+2} \\
 & - (j+s+2)(F_\xi)_{d,j+s+2} - |j-s|(F_\xi)_{d,j-s} \quad (B13)
 \end{aligned}$$

$$(F_\xi)_{pq} = \frac{1}{(p^2/\alpha + q^2\alpha)^2} \sum_m \sum_n \sum_k \sum_l B_{pqmnkl} \xi[W_{mn} W_{kl}] \quad (B14)$$

$$A'_1(d) = \frac{\partial A_1}{\partial W_{ij}} = C(m+r+2) F'_{m+r+2,d} + C(m-r) F'_{m-r,d} \\ - C(m+r) F'_{m+r,d} - C(m-r+2) F'_{m-r+2,d} \quad (B15)$$

$$A'_2(d) = \frac{\partial A_2}{\partial W_{ij}} = C(m+r-2) F'_{m+r-2,d} + C(m-r) F'_{m-r,d} \\ - C(m+r) F'_{m+r,d} - C(m-r-2) F'_{m-r-2,d} \quad (B16)$$

$$A'_5(d) = \frac{\partial A_5}{\partial W_{ij}} = (n+s) F'_{d,n+s} + |n-s-2| F'_{d,n-s-2} \\ - (n+s-2) F'_{d,n+s-2} - |n-s| F'_{d,n-s} \quad (B17)$$

$$A'_6(d) = \frac{\partial A_6}{\partial W_{ij}} = (n+s) F'_{d,n+s} + |n-s+2| F'_{d,n-s+2} \\ - (n+s+2) F'_{d,n+s+2} - |n-s| F'_{d,n-s} \quad (B18)$$

$$F'_{pq} = \frac{1}{(p^2/a+q^2a)^2} \sum_k \sum_l (B_{pqijkl} + B_{pqklij}) \xi[W_{mn} W_{kl}] \quad (B19)$$

$$\alpha = a/b \quad (B20)$$

$$C_1 = \begin{cases} 2 & \text{for } s = 1 \\ 1 & \text{for } s \neq 1 \end{cases}$$

$$C_2 = \begin{cases} 2 & \text{for } r = 1 \\ 1 & \text{for } r \neq 1 \end{cases}$$

$$C(k) = \begin{cases} 2 & \text{for } k = 0 \\ 1 & \text{for } k \neq 0 \end{cases}$$

$$W_{mn} = 0 \quad \text{for } m \text{ or } n < 1 \quad (B21)$$

and $\overline{[W_{mn} W_{kl}]}$ is the covariance matrix of the generalized displacements.

The diagonal terms of $\overline{[W_{mn} W_{kl}]}$ are the mean-square displacements $\overline{W_{mn}^2}$.

Expression for $(K_{rsij})_3$ which is similar to $(K_{rsij})_1$ has also been derived.

REFERENCES

1. J. Soovere, "The Effect of Acoustic-Thermal Environments on Advanced Composite Fuselage Panels," 24th Structures, Structural Dynamics and Materials Conference, Lake Tahoe, NV, May 1983, pp. 466-472.
2. J. Soovere, "Sonic Fatigue Testing of an Advanced Composite Aileron," Journal of Aircraft, Vol. 19, April 1982.
3. I. Holehouse, "Sonic Fatigue Design Techniques For Advanced Composite Aircraft Structures," AFWAL-TR-80-3019, AF Wright Aeronautical Laboratories, WPAFB, OH, April 1980.
4. C. Mei, "Large Amplitude Response of Complex Structures Due to High Intensity Noise," AFFDL-TR-79-3028, AF Flight Dynamics Laboratory, WPAFB, OH, April 1979.
5. M. J. Jacobson, "Sonic Fatigue Design Data for Bonded Aluminum Aircraft Structures," AFFDL-TR-77-45, WPAFB, OH, 1977.
6. R. C. W. Van der Heyde, and D. L. Smith, "Sonic Fatigue Resistance of Skin-Stringer Panels," AFFDL-TM-73-149-FYA, WPAFB, OH, 1974.
7. M. J. Jacobson, "Advanced Composite Joints; Design and Acoustic Fatigue Characteristics," AFFDL-TR-71-126, WPAFB, OH, 1972.
8. L. D. Jacobs, and D. R. Lagerquist, "Finite Element Analysis of Complex Panel to Random Loads," AFFDL-TR-68-44, WPAFB, OH, 1968.
9. G. E. Fitch, T. R. Dutko, L. M. Brennan, A. G. Tipton, P. M. Belcher, P. Wang, and P. A. Clawson, "Establishment of the Approach to, and Development of Interim Design Criteria for Sonic Fatigue," ASD-TDR-62-26, WPAFB, OH, 1962.
10. K. R. Wentz, D. B. Paul, and C. Mei, "Large Amplitude Random Response of Symmetric Laminated Composite Plates," Shock and Vibration Bulletin 52, May 1982, pp. 99-111.
11. C. Mei, "Response of Nonlinear Structural Panels Subjected to High Intensity Noise," AFWAL-TR-80-3018, AF Wright Aeronautical Laboratories, WPAFB, OH, March 1980.
12. C. Mei, and K. R. Wentz, "Analytical and Experimental Nonlinear Response of Rectangular Panels to Acoustic Excitation," 23rd Structures, Structural Dynamics and Materials Conference, New Orleans, LA, May 1982, pp. 514-520.
13. H. F. Wolfe, and K. R. Wentz, "Acoustic Fatigue Test Evaluation of Adhesively Bonded Aluminum Fuselage Panels using FM73/BR126 Adhesive/Primer System," 24th Structures, Structural Dynamics and Materials Conference, Lake Tahoe, NV, May 1983, pp. 626-631.

14. R. G. White, "Comparison of the Statistical Properties of the Aluminum Alloy and CFRP Plates to Acoustic Excitation," J. Composites, Oct. 1978, pp. 251-258.
15. S. Timoshenko, and S. Woinowsky-Krieger, "Theory of Plates and Shells," McGraw-Hill, 415-428, 1959.
16. H. N. Chu, and G. Herrmann, "Influence of Large Amplitudes on Free Flexural Vibrations of Rectangular Elastic Plates," J. Applied Mechanics, Vol. 23, December 1956, pp. 532-540.
17. R. E. Herbert, "Random Vibrations of Plates with Large Amplitude," J. Applied Mechanics, Vol. 32, Sept. 1965, pp. 547-552.
18. Y. K. Lin, "Response of a Nonlinear Flat Panel to Periodic and Randomly-Varying Loadings," J. Aerospace Sci., Sept. 1962, pp. 1029-1033, p. 1066.
19. S. Levy, "Bending of Rectangular Plates with Large Deflections," NACA Report 737, 1942.
20. D. B. Paul, "Large Deflections of Clamped Rectangular Plates with Arbitrary Temperature Distributions," AFWAL-TR-81-3003, Volume I, AF Wright Aeronautical Laboratories, WPAFB, OH, Feb. 1982.
21. A. S. Volmir, "Flexible Plates and Shells," AFFDL-TR-66-127, AF Flight Dynamics Laboratory, WPAFB, OH, April 1967.
22. P. T. D. Spanos, and W. D. Iwan, "On the Existence and Uniqueness of Solutions Generated by Equivalent Linearization," Int. J. Nonlinear Mech., Vol. 13, 1978, pp. 71-78.
23. T. S. Atalik, and S. Utku, "Stochastic Linearization of Multi-Degree-of-Freedom Nonlinear Systems," Earthquake Eng. Struct. Dyn., Vol. 4, 1976, pp. 411-420.
24. W. D. Iwan, and I. M. Yang, "Application of Statistical Linearization Technique to Nonlinear Multidegree-of-Freedom Systems," J. Applied Mechanics, Vol. 39, June 1972, pp. 545-550.
25. T. K. Caughey, "Nonlinear Theory of Random Vibrations," in Advances in Applied Mechanics, Edited by C. S. Yih, Vol. 11, Academic Press, 1971, pp. 209-253.
26. E. T. Foster, Jr., "Semilinear Random Vibrations in Discrete Systems," J. Applied Mechanics, Vol. 35, Sept. 1968, pp. 560-564.
27. T. K. Caughey, "Equivalent Linearization Techniques," JASA, Vol. 35, 1963, pp. 1706-1711.
28. N. Krylov, and N. Bogoliubov, "Introduction to Nonlinear Mechanics," translated by Lefshletz, S. in Annals of Mathematical Studies, No. 11, Princeton University Press, N. J., 1943.

29. F. F. Rudder, Jr. and H. E. Plumblee, Jr., "Sonic Fatigue Design Guide for Military Aircraft," AFFDL-TR-74-112, AF Flight Dynamics Laboratory, WPAFB, OH, May 1975, p. 265-266.